JOC The Journal of Organic Chemistry

Article

pubs.acs.org/joc

Photochemical Formation of Anthracene Quinone Methide Derivatives

Đani Škalamera,[†] Kata Mlinarić-Majerski,[†] Irena Martin Kleiner,[‡] Marijeta Kralj,[‡] Jessy Oake,[§] Peter Wan,[§] Cornelia Bohne,[§] and Nikola Basarić*[,†]

[†]Department of Organic Chemistry and Biochemistry and [‡]Division of Molecular Medicine, Ruđer Bošković Institute, Bijenička cesta 54, 10 000 Zagreb, Croatia

[§]Department of Chemistry, University of Victoria, Box 1700 STN CSC, Victoria BC V8W 2Y2, Canada

Supporting Information

ABSTRACT: Anthrols **2**−**7** were synthesized and their photochemical reactivity investigated by irradiations in aq CH_3OH. Upon excitation with visible light (λ > 400 nm) in methanolic solutions, they undergo photodehydration or photodeamination and deliver methyl ethers, most probably via quinone methides (QMs), with methanolysis quantum efficiencies Φ_R = 0.02−0.3. Photophysical properties of **2**−**7** were determined by steady-state fluorescence and time-correlated single photon counting. Generally, anthrols **2**−**7** are highly fluorescent in aprotic solvents (Φ_F = 0.5−0.9), whereas in aqueous solutions the fluorescence is quenched due to excited-state proton transfer (ESPT) to solvent. The exception is amine **4** that undergoes excited-state intramolecular proton transfer (ESIPT) in neat CH_3CN where photodeamination is probably coupled to ESIPT. Photodehydration may take place via ESIPT (or ESPT) that is coupled to dehydration or via a hitherto undisclosed pathway that involves photoionization and deprotonation of radical cation, followed by homolytic cleavage of the alcohol OH group from the phenoxyl radical. QMs were detected by laser flash photolysis and their reactivity with nucleophiles investigated. Biological investigation of **2**−**5** on human cancer cell lines showed enhancement of antiproliferative effect upon exposure of cells to irradiation by visible light, probably due to formation of electrophilic species such as QMs.

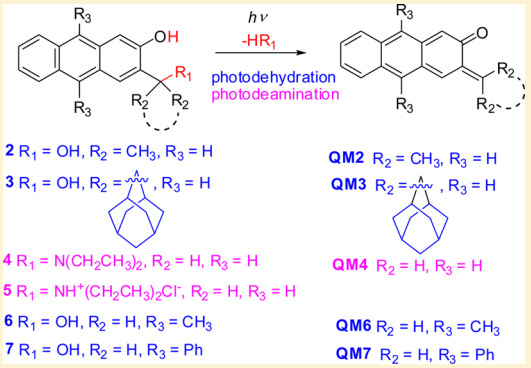

INTRODUCTION

Quinone methides (QMs) are important reactive intermediates in the chemistry and photochemistry of phenols.[1] For example, the activity of some antineoplastic antibiotics such as mitomycin is based on metabolic formation of QMs (via initial reduction to the phenol) that alkylate DNA.[2−4] Therefore, the biological role of QMs[5−7] has mainly been connected to their reactivity with nucleobases[8−10] and DNA.[11−14] However, QMs also react with amino acids[15,16] and proteins.[17] We have recently demonstrated that antiproliferative activity of photogenerated anthracene QMs stems from their reaction with intracellular proteins rather than with DNA.[18]

The most convenient approach for the preparation of QMs in biological systems relies on photochemical methods[19,20] that include photodeamination from the Mannich salts of the corresponding phenols[16,21−23] or photodehydration of the corresponding benzyl alcohols.[24,25] Photodeamination of Mannich salts has recently been applied in the investigation of biological activity of QMs,[26,27] and the ability of naphthalenediimide QM derivatives to selectively target guanine quadruplex structures has been demonstrated.[28−30] Photodeamination can also be triggered by an intramolecular photoinduced electron-transfer reaction with naphthalene diimide as photooxidant.[31] Although a number of methods for the efficient generation of QMs exist, reports on biological effects of simple QMs are scarce due to their high reactivity and short lifetimes. QMs cannot be stored; they have to be generated in situ. A further drawback for their photochemical formation is the use of short-wavelength UV light which is not applicable in biology, and particularly not in medicine. However, Freccero et al.[23,32] and our laboratory[33] have recently reported examples of QM photogeneration by use of near-visible light. Thus, anthrol **1** can be excited at λ > 400 nm delivering **QM1**. The QM is protonated to $\mathbf{1}^+$, and subsequently in a reaction with nucleophiles gives adducts (Scheme 1).[33] Preliminary biological investigation indicated enhancement of antiproliferative activity for the human cancer cells when irradiated, suggesting that the effect is due to intracellular photochemical formation of **QM1** or $\mathbf{1}^+$.[33]

Prompted by these preliminary results with anthrol **1**,[33] we report here a systematic study of the photochemical reactivity for the photodehydration or photodeamination of anthrols **2**−**7**, and we investigated their antiproliferative activity upon irradiation. Anthrol derivatives **2**−**7** were all substituted at the anthracene positions 2 and 3. Compounds **2** and **3** bear methyl

Received: November 13, 2016
Published: May 23, 2017

DOI: 10.1021/acs.joc.6b02735
J. Org. Chem. 2017, 82, 6006−6021

Scheme 1

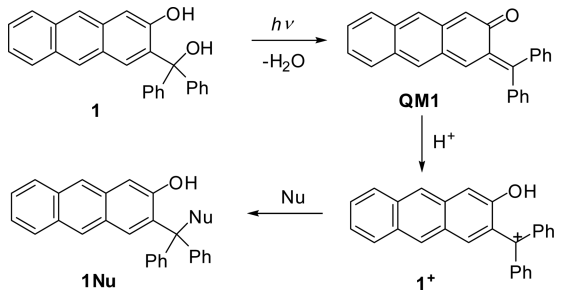

or adamantyl substituents at the hydroxymethyl group which are known to increase the quantum yield for photodehydration[34] and enhance antiproliferative effects.[35−37] Compounds **4** and **5** are methylamine derivatives that are anticipated to undergo more efficient formation of QMs in deamination reactions.[22] Moreover, positively charged anthracene **5** may intercalate into DNA and thus enhance the aptitude for alkylation of photogenerated QMs.[14] Anthrols **6** and **7** are substituted at the anthracene positions 9 and 10 to increase their photochemical stability with respect to photooxidations and render them more fluorescent. It was anticipated that the corresponding QMs from **6** and **7** may also be fluorescent, which would make their detection easier. Photochemical reactivity was studied by preparative irradiations in the presence of CH_3OH as a nucleophile. Fluorescence properties and singlet excited-state reactivity were investigated by steady-state and time-resolved fluorescence, whereas for the detection of reactive intermediates, laser flash photolysis was used. For compounds **2**−**5**, antiproliferative activity was tested on three human cancer cell lines with and without irradiation. Enhancement of the antiproliferative effect for the irradiated cells is probably due to photochemical formation of anthracene QMs in photodehydration and photodeamination reactions. Most importantly, detailed mechanistic investigation unraveled a possible new pathway for the QM formation that involves photoionization and a homolytic cleavage of the OH group.

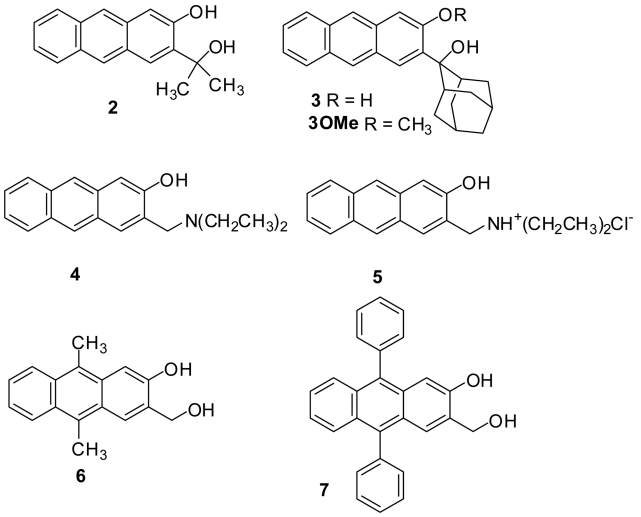

RESULTS

Synthesis. The synthesis of anthrols **2**−**5** started from the commercially available 2-aminoanthraquinone, which was converted to 2-hydroxyanthraquinone (**8**) via a known procedure.[38] Bromination of **8** with excess of bromine afforded a mixture of 3-bromo-2-hydroxyanthraquinone (**9**) and 1,3-dibromo-2-hydroxyanthraquinone (**10**). The mixture was subjected to a reduction with $NaBH_4$ in alkaline aqueous solution (1 M Na_2CO_3) to yield pure 2-bromo-3-anthrol (**11**). Under these conditions, selective debromination occurs on the anthracene position 1, whereas debromination on the position 3 is insignificant if the reduction is not run longer than 15 min. Thus, **11** was obtained selectively, in high yield (95%) and with high purity. This modification significantly improved our previous procedure[33] for the preparation of **11** by increasing the yield over two steps with no need for chromatography. In the next step, **11** was treated with an excess of BuLi according to the procedure developed by Freccero et al.[26] on similar systems, which avoids the use of a protecting group on the phenolic OH. The lithiated compound reacted with DMF to afford the corresponding aldehyde **12** (Scheme 2).

Anthrols **3** and **4** were prepared from bromoanthrol **11**, which was treated with excess BuLi, and then organolithium compound was quenched with acetone or 2-adamantanone (Scheme 3). We also prepared methyl ether **3OMe** by a simple methylation of **3** with CH_3I in basic conditions (K_2CO_3).

Ethylamine derivative **4** was obtained from carbaldehyde **12** in a reductive amination and subsequently transformed to hydrochloride salt **5** (Scheme 4).

Synthesis of anthrols **6** and **7** started from antraquinone **9**.[33] Treatment with an excess of MeLi or PheLi followed by reduction gave methylated anthrol derivative **13-Me** or phenyl derivative **13-Ph**. Compounds **13** in a reaction with BuLi and quenching with DMF afforded carbaldehydes **14-Me** or **14-Ph** that were reduced to alcohols **6** or **7**, respectively (Scheme 5).

Photochemistry. On the basis of literature precedent,[22,24,33] it is expected that irradiation of anthrols **2**−**7** in CH_3OH−H_2O would give photomethanolysis products via QM intermediates. Preparative irradiations of **2**−**7** were conducted by irradiating CH_3OH−H_2O (4:1) solutions at 350 nm and by analyzing the composition of the solutions by HPLC (see Figures S1−S4 in the Supporting Information). Methanolysis reactions of **2**, **3**, **6**, and **7** run to high conversions of 80−90% afforded cleanly methyl ether products **15**, **16**, **18**, and **19**, respectively (Scheme 6). However, irradiation of **4** and **5** gave methyl ether **17** formed as the major product, and small amounts of alcohol (1−5%) were detected by HPLC (see Figures S3 and S4 in the Supporting Information). Irradiations of **2** and **3** at different H_2O concentrations gave the same products **15** and **16** irrespective of H_2O content. Although a clear trend cannot be seen with **2**, photomethanolysis is generally more efficient at higher H_2O concentration, due to faster phenol deprotonation from S_1 to H_2O clusters then to CH_3OH.[39−42] Water concentration had no influence on the efficiency of photomethanolysis of **4**, whereas for **5**, a higher methanolysis efficiency was observed at higher H_2O concentration, in accord with precedent literature.[22] Photomethanolysis was also conducted by irradiating anthrols in CH_3OH−H_2O (4:1) by use of lamps with the output at 420 nm or "cool white" light where the same products **15**−**19** were obtained. Excitation of **2**−**7** by near-visible light is particularly important for the applicability in biological systems.

The efficiency of photomethanolysis (Φ_R) for **2**−**5** was determined by the simultaneous use of three actinometers, ferrioxalate (Φ_{254} = 1.25),[43,44] KI/KIO_3 (Φ_{254} = 0.74),[43,45] and valerophenone (Φ_{254} = 0.65 ± 0.03),[43,46] as we already described for **1**.[33] For **6** and **7**, only KI/KIO_3 was used, since

DOI: 10.1021/acs.joc.6b02735
J. Org. Chem. 2017, 82, 6006−6021

Scheme 2

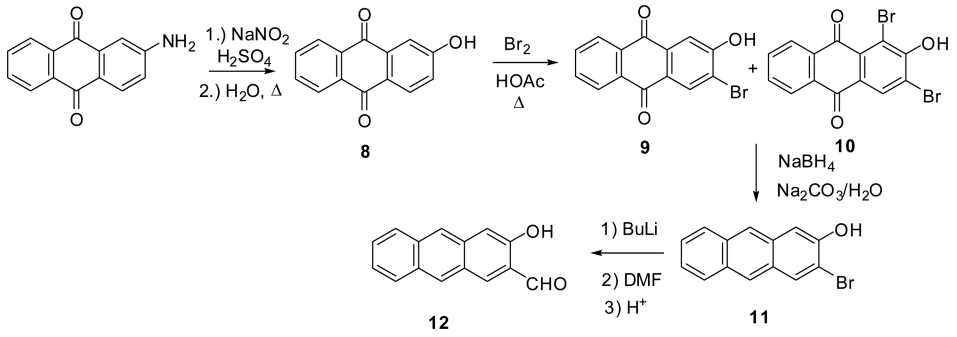

Scheme 3

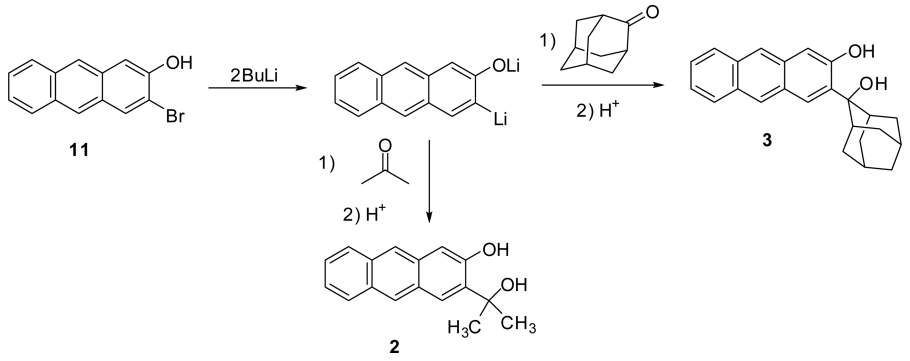

Scheme 4

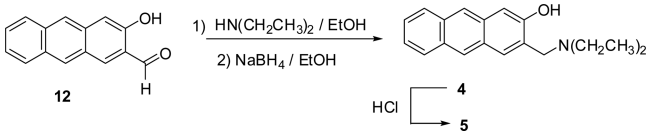

Scheme 5

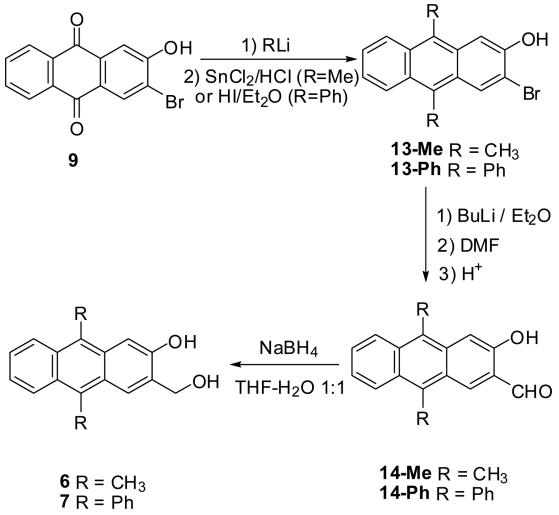

Scheme 6

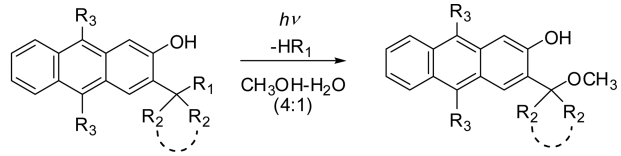

2 R_1 = OH, R_2 = CH_3, R_3 = H
3 R_1 = OH, R_2 = , R_3 = H
4 R_1 = $N(CH_2CH_3)_2$, R_2 = H, R_3 = H
5 R_1 = $NH^+(CH_2CH_3)_2Cl^-$, R_2 = H, R_3 = H
6 R_1 = OH, R_2 = H, R_3 = CH_3
7 R_1 = OH, R_2 = H, R_3 = Ph

15 R_2 = CH_3, R_3 = H
16 R_2 = , R_3 = H
17 R_2 = H, R_3 = H
18 R_2 = H, R_3 = CH_3
19 R_2 = H, R_3 = Ph

consistent results were obtained as for **2**–**5** with three actinometers. The measured values of Φ_R are compiled in Table 1. Comparison of Φ_R for phenyl **1** and methyl derivative **2** indicates that the introduction of the substituents to the methyl group decreased the reaction efficiency. On the contrary, the highest Φ_R was observed for the adamantyl derivative **3**. The adamantyl group probably increases the stability of the corresponding QM and thus enhances the methanolysis reaction efficiency. An analogous trend has already been observed in similar phenyl[34] and naphthyl derivatives.[37] Furthermore, the efficiency Φ_R in the photodeamination from **5** is less efficient than elimination of the amine, contrary to previous report with simple cresol derivatives.[22] The observation may be explained by different electronic influence of the ethylamine or ethylammonium group to the photophysical properties of anthrol.

It is known that QMs react with electron-rich alkenes in Diels–Alder reaction to give chromanes.[25,47−49] However, irradiations of **2**–**7** in neat CH_3CN or aqueous CH_3CN in the presence of ethyl vinyl ether (EVE) did not give chromane adducts, probably due to slow kinetics of the Diels–Alder reaction (vide infra). Thus, photochemistry of anthrols cannot be exploited further in different applications, as elegantly demonstrated for naphthol derivatives by Popik et al.[47,48,50]

DOI: 10.1021/acs.joc.6b02735
J. Org. Chem. 2017, 82, 6006−6021

Table 1. Photomethanolysis Quantum Yields (Φ_R) for 1−7[a]

compd	Φ_R
1	0.023 ± 0.001[b,c]
2	0.015 ± 0.001[b]
3	0.33 ± 0.01[b]
4	0.22 ± 0.01[b]
5	0.15 ± 0.01[b]
6	0.04 ± 0.01[d]
7	0.048 ± 0.009[d]

[a]Measurement conducted in CH_3OH-H_2O (4:1) at 254 nm. Measurements were done in triplicate, and the mean value is reported. The quoted error corresponds to the maximum absolute deviations. [b]Measured by simultaneous use of three actinometers, ferrioxalate (Φ_{254} = 1.25),[43,44] KI/KIO_3 (Φ_{254} = 0.74),[43,45] and valerophenone (Φ_{254} = 0.65 ± 0.03),[43,46] Φ_R was calculated according to eqs S1−S5 in the Supporting Information. [c]Value taken from ref 33. [d]Measured by use of a KI/KIO_3 actinometer.

Photophysical Properties. Photophysical properties of **2**−**7** are important for the understanding of their photochemical reactivity from the singlet excited state S_1. Absorption and fluorescence spectra were measured in CH_3CN and CH_3CN-H_2O (1:1) (for absorption and fluorescence spectra see Figures S5−S24 in the Supporting Information). The absorption spectra of **2**, **3**, **6**, and **7** in CH_3CN and CH_3CN-H_2O are characterized by a band at 310−420 nm, corresponding to $S_0 \rightarrow S_1$ transition. Thus, anthrol derivatives can be excited with near-visible light (>400 nm), which is important for biological applications. Amine derivatives **4** and **5** were not soluble in neat CH_3CN at the concentrations for molar absorption coefficient measurements, but are soluble in neutral CH_3CN-H_2O. In aqueous solution, **4** and **5** have a band in the absorption spectrum at 310−420 nm and a shoulder stretching to 500 nm which is attributed to the phenolate of these compounds (Figures S12 and S18 in the Supporting Information). The pK_a of the phenolic OH is probably significantly lowered by the presence of the *o*-methylammonium group, as seen with cresol derivatives.[22] Thus, in the neutral aqueous solution the ethylamine is protonated to give **5**, and phenol **5** is in equilibrium with zwitterionic phenolate **4zw** (Scheme 7).

Scheme 7

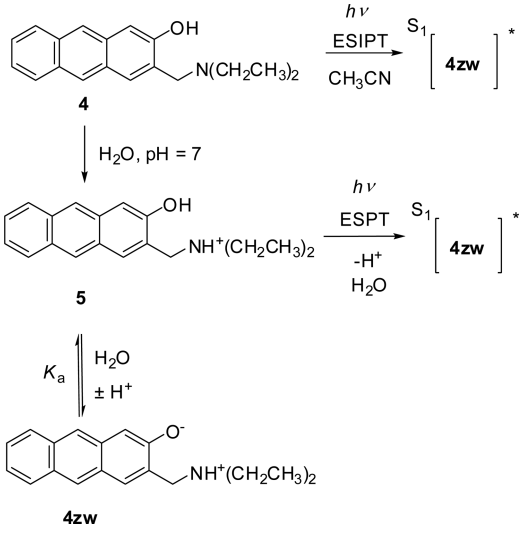

Fluorescence spectra of **2** and **3** in CH_3CN have bands at 400−500 nm, and the quantum yields are high, $\Phi_F \approx 0.8$ (Table 2). The fluorescence decay was fit to a monoexponential function with relatively long S_1 lifetimes ($\tau \approx 20$ ns). Substituted anthracenes **6** and **7**, as well as ammonium salt **5**, have similar fluorescence spectra with maxima at 400−500 nm (Figure 1). They are also highly fluorescent with Φ_F = 0.5−0.9, but their fluorescence decays could not be fit to a single exponential function. Global analysis of the fluorescence decays collected over different wavelengths revealed two decay lifetimes (see eq S7, Table S1, and Figures S26 and S27 in the Supporting Information). For anthrols **5**−**7**, these probably correspond to two conformers, as seen with 2-methoxyanthracene.[51]

Ammonium derivative **4** in neat CH_3CN has different fluorescence properties than observed for the other anthrols. It exhibits typical dual fluorescence, with an additional band at 575 nm attributed to the phenolate emission. The assignment of the bands in the fluorescence spectra is based on experiments in the presence of acid or base. In the presence of H_2SO_4 only the band at 400−500 nm is observed, whereas upon addition of triethylamine the band at 575 nm becomes stronger (see Figure S16 in the Supporting Information). The presence of phenolate is also apparent in the absorption spectrum. Therefore, the relative ratio of the fluorescence intensity from the phenol and the phenolate, as well as the Φ_F value, depend on the excitation wavelength (see Figures S14 and S15 in the Supporting Information). The equilibrium between the phenol and the phenolate is temperature dependent with higher phenolate content present at a lower temperature (see Figure S17 in the Supporting Information). The fluorescence decay for **4** in CH_3CN was fit to a sum of two exponentials with the decay lifetimes corresponding to the phenol (2.2 ns) and phenolate (16.3 ns), both with positive pre-exponential factors suggesting that phenolate is formed in the ground state (Table S2 in the Supporting Information). In addition to the phenolate in equilibrium in S_0, it is probably also formed in S_1 by ESIPT due to the enhanced acidity of phenol in S_1 and the proximity of the basic amine (Scheme 7). Therefore, Φ_F for **4** in CH_3CN is much lower than for the other anthrols.

Addition of H_2O to the CH_3CN solutions of anthrols significantly quenched the fluorescence for all anthrols except for amine **4** and methoxy derivative **3OMe**. In addition to fluorescence quenching, in all cases except for **3OMe** typical dual fluorescence was observed with two emission bands, at 450 and 575 nm, attributed to the phenol and phenolate, respectively. The methoxy derivative does not exhibit dual fluorescence since it does not have a phenolic OH. Furthermore, anthrol **4** is an exception that has higher Φ_F in aqueous solution. Namely, in neutral aqueous solution the amine is protonated, which blocks the efficient ESIPT pathway from taking place in neat CH_3CN. Thus, in neutral aqueous solution **4** and **5** have the same fluorescence properties. Phenolates are formed in S_1 in the aqueous solution by ESPT to solvent, as indicated by single-photon-counting (SPC) measurements where the kinetics were fit to a sum of two or more exponentials with negative pre-exponential factors for kinetics collected at longer wavelengths where the phenolates emit, consistent with a growth kinetics for the formation of the phenolate (for kinetic schemes,[53,54] see Scheme S1, eqs S7−S10, and pre-exponential factors Table S1 in the Supporting Information). We collected time-resolved fluorescence spectra for anthrol **7** with the highest Φ_F in order to obtain more

DOI: 10.1021/acs.joc.6b02735
J. Org. Chem. 2017, 82, 6006−6021

Table 2. Photophysical Properties of Anthracenes 1−7

	$\Phi_F(CH_3CN)$[b]	$\Phi_F(CH_3CN-H_2O)$[b]	τ (CH_3CN)[c] (ns)	τ (CH_3CN-H_2O)[c,d] (ns)
1[a]	0.86 ± 0.01	0.39 ± 0.01	17.8 ± 0.1	1.7 ± 0.2 (growth)[f]
				8.1 ± 0.2 (growth)
				24.5 ± 0.1 (decay)
2	0.80 ± 0.05	0.54 ± 0.02	23.6 ± 0.2	3.7 ± 0.1 (growth)[f]
				13.8 ± 0.1 (growth)
				20.8 ± 0.1 (decay)
3	0.79 ± 0.01	0.29 ± 0.02	21.8 ± 0.1	2.1 ± 0.1 (growth)[f]
				10.1 ± 0.1 (growth)
				19.8 ± 0.1 (decay)
3OMe	0.85 ± 0.05		21.1 ± 0.1	26.9 ± 0.1
4	0.10 ± 0.03[e]	0.27 ± 0.06[e]	2.3 ± 0.3[f]	1.9 ± 0.1 (growth)[f]
			16.3 ± 0.1	7.2 ± 0.1 (growth)
				23.1 ± 0.1 (decay)
5	0.45 ± 0.05	0.25 ± 0.06[e]	9.0 ± 0.1[f]	2.0 ± 0.1 (growth)[f]
			27.3 ± 0.1	5.7 ± 0.1 (growth)
				23.0 ± 0.1 (decay)
6	0.52 ± 0.02	0.30 ± 0.02	17.3 ± 0.1[f]	8.0 ± 0.1 (growth)[f]
			20.4 ± 0.1	16 ± 3 (decay)
7	0.92 ± 0.02	0.25 ± 0.02	13.4 ± 0.1[f]	4.5 ± 0.1 (growth)[f]
			14.3 ± 0.1	18.2 ± 0.1 (decay)

[a]Taken from ref 33. [b]Quantum yields of fluorescence (Φ_F) were measured by use of quinine sulfate in 0.05 M aqueous H_2SO_4 (Φ_F = 0.55) as a reference.[52] An average value is reported from a single experiment by excitation at three wavelengths. The errors quoted correspond to maximum absolute deviations (see the Experimental Section). [c]Singlet excited-state lifetimes were obtained by global fitting of fluorescence decays measured at several wavelengths by time-correlated single photon counting (see the Experimental Section). [d,a]"Growth" and "decay" indicate the type of kinetics at the emission wavelengths for the phenolate. [e]Depends on the excitation wavelength (increases with λ). [f]For details on fitting and pre-exponential factors that depend on the detection wavelength, see Tables S1 and S2.

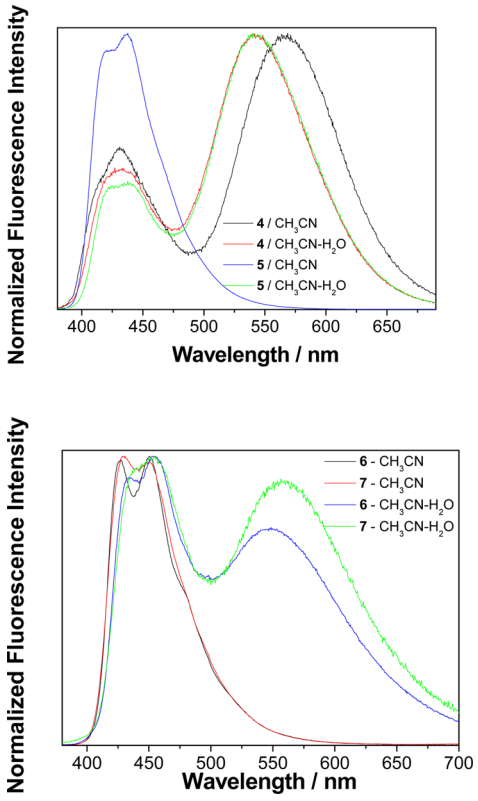

Figure 1. Normalized fluorescence spectra (λ_{exc} = 370 nm) of **4** and **5** (top) and **6** and **7** (bottom) in CH_3CN or CH_3CN-H_2O (1:1).

information on the decay processes involving S_1. The spectra are in accord with the phenol emitting at short delays after excitation and the phenolate present at longer delays (see Figure S24 in the Supporting Information).

The fluorescence decays for anthrols **1−5** in aqueous solution were fit to a sum of three exponentials where at the emission wavelength for the phenolate two growing components with negative pre-exponential factors were observed which correspond to the two shorter lived species. We propose that these two short-lived species correspond to two conformers of anthrol that deprotonate in S_1 with different rate constants (see Scheme S2, an example of decay Figure S27, and pre-exponential factors Table S2 in the Supporting Information). One anthrol conformer gives phenolate by ESPT to solvent, whereas the other anthrol could undergo ESPT to solvent and ESIPT, giving also zwitterionic phenolate and leading eventually to dehydration and QM formation. The other plausible assignment for the two short-lived species may be due to the presence of phenols with a different number of associated H_2O molecules that deprotonate in S_1 with different rate constants. Namely, it is known that several H_2O molecules are necessary as proton-accepting species in ESPT, giving rise to nonlinear quenching of fluorescence by H_2O.[55] We do not have sufficient information from the time-resolved studies to differentiate between these two possibilities.

The solution pH should in principle be controlled for ESPT reactions. That is why some measurements were conducted in the presence of phosphate buffer (c = 0.1 M) at pH 7.0 (particularly those corresponding to compounds **6** and **7**). However, the results were not different from the cases when the solutions were not buffered. We have demonstrated on some other molecules undergoing dehydration that the efficiency for the QMs formation is pH-independent over a wide pH range (pH 3−9).[34−37] For the deamination reaction, QM formation depends on the prototropic form of the molecule, being the

DOI: 10.1021/acs.joc.6b02735
J. Org. Chem. 2017, 82, 6006−6021

most efficient reaction when the molecule is in the zwitterionc form (at pH > 9).[22] Thus, under near-neutral conditions, no influence of pH is expected to the kinetics of QM formation. Moreover, hydration of QMs is acid and base catalyzed but in the wide near-neutral pH region the reaction is pH independent.[25,56,57]

Laser Flash Photolysis (LFP). LFP experiments were conducted for **2**–**7** to probe for the formation of QMs, carbocations or other reactive intermediates of biological relevance. The transient absorption spectra were measured by excitation at 355 nm with a Nd:YAG laser in CH_3CN and CH_3CN–H_2O, where different behavior was anticipated due to the presence or not of ESPT pathways. Moreover, the measurements were conducted in N_2- and O_2-purged solutions, where O_2 is expected to quench some transient species (triplets and radicals) shortening their lifetimes, while QMs and carbocations should not be affected since they do not react with oxygen (for the transient absorption spectra, decays, and quenching plots, see Figures S28–S64 in the Supporting Information).

In both N_2- and O_2-purged CH_3CN solutions of **2**, a transient was detected with a maximum at 690 nm that did not decay with first-order kinetics (Figure 2 top). In O_2-purged

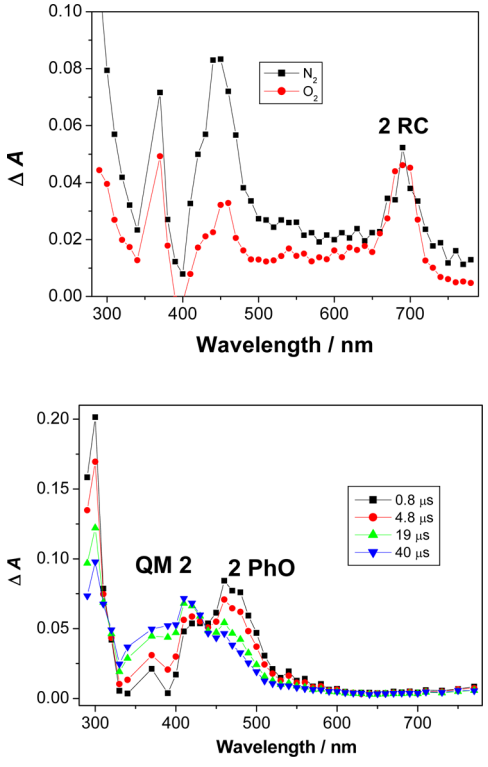

Figure 2. Transient absorption spectra of **2** in N_2- and O_2-purged CH_3CN (top) collected ~2 μs after the laser pulse and O_2-purged CH_3CN–H_2O (bottom).

solution, the transient was fit to a sum of two exponentials with $k \approx 2.2 \times 10^6$ s^{-1} ($\tau = 0.45 \pm 0.05$ μs) and $k \approx 4.1 \times 10^5$ s^{-1} ($\tau \approx 2.4$ μs, for the details on fitting see Figures S29–S31 in the Supporting Information). The longer lived transient was quenched with CH_3OH and H_2O, but the rate constant for the quenching could not be estimated due to the nonlinear dependence of k_{obs} on concentration (see Figure S32 in the Supporting Information). In aqueous solution, the transient at 700 nm cannot be detected because its lifetime is shorter than the detection limit of the setup used. Based on the quenching with CH_3OH and H_2O and comparison with precedent spectra,[58,59] the transient with the lifetime of 2.4 μs was assigned to radical cation **2RC**, but we cannot give a firm assignment for the short-lived transient ($\tau = 0.45$ μs). It cannot correspond to the triplet excited state, C-centered radical, or solvated electron because the measurement was performed in oxygenated CH_3CN where these transients would be quenched. Moreover, it cannot be the phenoxyl radical, which is expected to absorb at shorter wavelengths.[60,61] The assignment of this transient is beyond the scope of this report focused on QM formation, and no further attempts for its identification were made. In aqueous solutions, the phenol radical cations deprotonate to give phenoxyl radicals.[62] Methanol or H_2O are not typical quenchers that react in a bimolecular reaction with radical cations. Since several molecules are required as proton-accepting species,[55,63] nonlinear quenching plots of the transient were observed. Furthermore, in CH_3CN and CH_3CN–H_2O solutions of **2**, additional transients were detected between 350 and 600 nm. Thus, in the O_2-purged aqueous solution of **2** (Figure 2, bottom) at short delays after the laser pulse, a transient was observed at 480 nm, where the decay ($k \approx 9 \times 10^4$ s^{-1}) matched with the rise of another transient absorbing at shorter wavelengths 350–400 nm. This latter transient decays over the millisecond time scale, $\tau \approx$ 200–300 ms (see Figure S34 in the Supporting Information). Popik et al. also detected two transients in a naphthalene series (from 3-(hydroxymethyl)-2-naphthol) and explained this observation by the formation of naphthalene benzoxete **NBO** that undergoes rearrangement to quinone methide **NQM**.[25] However, anthracene benzoxete derivative **ABO2** cannot absorb light at 450–550 nm because it contains only the anthracene chromophore. Therefore, we tentatively assigned the short-lived transient with a maximum at 480 nm to phenoxyl radical **2PhO**, based on the position of the absorption maximum and decay kinetics from precedent literature.[60,61] Precise decay kinetics for the long-lived transient could not be revealed with the setup used, precluding quenching studies to confirm the assignment of this transient. We tentatively assign it to **QM2** since the methanolysis experiments strongly indicated the formation of this transient. LFP experiments for **2** were also conducted in 2,2,2-trifluoroethanol (TFE), in which electrophilic species such as QMs[64,34,36] and carbocations[65,66] exhibit long lifetimes due to the polar non-nucleophilic character of the solvent (see Figure S36 in the Supporting Information). However, the spectra did not differ from those measured in aqueous CH_3CN. Contrary to **1**, formation of **QM2** and the corresponding carbocation could not be time-resolved.

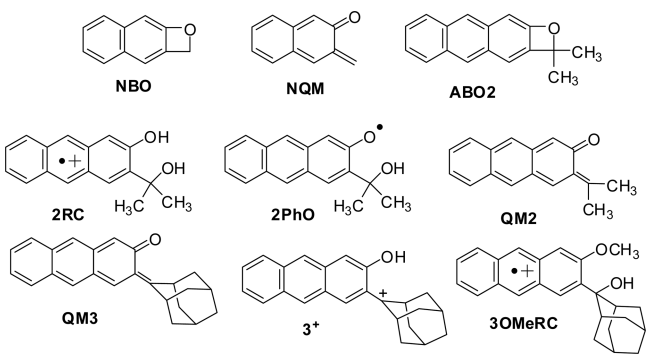

DOI: 10.1021/acs.joc.6b02735
J. Org. Chem. 2017, 82, 6006–6021

Transient absorption spectra of **3** in CH_3CN and CH_3CN-H_2O solution resemble those of **2**. In the CH_3CN solution we detected the radical cation (λ_{max} = 700 nm, τ = 950 ± 50 ns) and solvated electron, which was also detected in the O_2-purged aqueous solution (λ = 700 nm, $\tau \approx$ 50 ns) where the radical cation rapidly deprotonates. Reported lifetimes for solvated electron in aqueous solution vary from 10 μs[67] to 300−500 μs.[68] Nevertheless, O_2 quenches the solvated electron with a rate constant of 2×10^{10} M^{-1} s^{-1},[69] so in O_2-purged aqueous solution the lifetime of hydrated electron should be ∼35 ns. Assignment of the transient at 700 nm to the radical cation is further supported by LFP experiments with **3OMe** (see Figure 3, top, and S43 in the Supporting Information), where the same

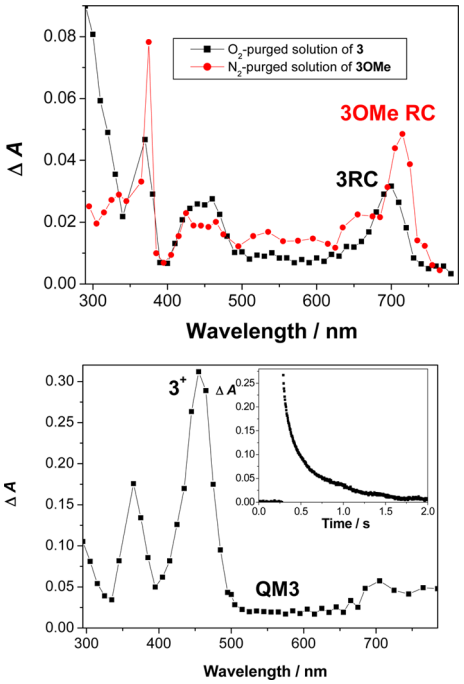

Figure 3. Transient absorption spectra of **3** and **3OMe** in O_2-purged CH_3CN or N_2-purged CH_3CN-H_2O (1:1) collected 700 ns after the laser pulse (top) and in 1,1,1,3,3,3-hexafluoroisopropanol (HFIP) collected 760 ns after the laser pulse (bottom, weak ΔA at 500−600 nm corresponds to **QM3**, whereas the maximum at 450 nm corresponds to 3^+; inset: decay of 3^+at 450 nm).

transient was detected in both CH_3CN (τ = 3.6 ± 0.1 μs) and CH_3CN-H_2O (τ = 50 ± 2 μs). Namely, **3OMeRC** cannot deprotonate to phenoxyl radical in H_2O since it has no free phenolic OH. On the contrary, for anthrol **3** in CH_3CN solution, the phenoxyl radical was detected at 300−500 nm ($\tau \approx$ 10 μs) together with a long-lived transient that has a lifetime of seconds that we tentatively assigned to **QM3**. LFP in TFE also did not provide any representative spectrum that could be assigned to QM. However, in 1,1,1,3,3,3-hexafluoroisopropanol (HFIP), **3** gave a strong transient with a maximum at 450 nm (Figure 3, bottom, and Figures S41 and S42 in the Supporting Information). The transient decayed with almost first-order kinetics to the baseline (k = 2.5 ± 0.5 s^{-1}, τ = 0.4 ± 0.1 s), and its decay became faster in the presence of nucleophiles CH_3OH or H_2O. However, the quenching rate constants could not be estimated due to a nonlinear dependence of k_{obs} with quencher concentration. At 500−600 nm, an additional weaker transient was observed that decayed much faster ($k = 3 \times 10^6$ s^{-1}, τ = 360 ± 30 ns). The transient absorbing at 500−600 nm was tentatively assigned to **QM3** based on the position of the absorption maxima and decay kinetics from precedent literature,[33] whereas the long-lived transient corresponds to adamantyl cation 3^+. Namely, the absorption spectrum of **3** in HFIP (see Figure S41 in the Supporting Information) indicated the presence of 3^+, which is formed in S_0 due to the high acidity of HFIP. However, excitation to S_1 increases the concentration of 3^+ by photoelimination of H_2O. It remains unclear whether H_2O photoelimination takes place via **QM3**, or cation 3^+ is directly formed in a HFIP acid-catalyzed pathway.

LFP experiments of **4** and **5** gave rise to short-lived transients absorbing over the whole visible part of the spectrum (see Figures S44−S51 in the Supporting Information). For example, in the N_2-purged CH_3CN solution of **4** the transient decayed with $k = (1.0 \pm 0.1) \times 10^7$ s^{-1} (τ = 100 ± 10 ns). Interestingly, O_2 and N_2O only weakly quenched the transient (O_2- or N_2O-purged CH_3CN $k = (1.3 \pm 0.1) \times 10^7$ s^{-1}, τ = 80 ± 5 ns), precluding its assignment to solvated electron or the triplet excited state. Transient absorption spectra of **5** looked the same as those for **4**, but the transient decayed faster (N_2- and O_2-purged CH_3CN, τ = 65 ± 5 ns). The short-lived transient was not quenched by nucleophiles such as CH_3OH, ethanolamine or NaN_3. On the contrary, the transient in H_2O lived longer (O_2-purged CH_3CN-H_2O, τ = 130 ± 10 ns). Although a firm assignment of the short-lived transients for **4** and **5** are not warranted at this point, we may tentatively say that these are anthracene radical ions formed by photoionization or electron transfer. Namely, the absorption properties of anthracene radical cations and radical anions are very similar.[70] Moreover, amines are known to form exciplexes with anthracenes wherein a polar solvent a complete charge transfer may lead to the formation of anthracene radical anions.[71] These fast components are not the focus of this study, which is the elucidation of mechanisms leading to the QM formation, and were not pursued further. In addition to the short-lived transient absorbing over the entire spectrum, a transient was detected from **4** and **5** in CH_3CN and CH_3CN-H_2O absorbing at 400−600 nm that was longer lived ($k \approx 1 \times 10^5$ s^{-1}, $\tau \approx$ 10 μs) and not affected by the addition of O_2. Based on the comparison with the transient absorption spectra of **2** and **3**, the longer lived transient at 400−600 nm probably corresponds to phenoxyl radical. LFP experiments in TFE gave the spectra with the same appearance as those measured in CH_3CN and CH_3CN-H_2O. Thus, the anticipated **QM4** formed in the photodeamination from **4** and **5** was not detected by LFP.

Transient absorption spectra from **6** and **7** are very similar to those of **2** and **3**. Thus, in an N_2-purged CH_3CN solution of **6**, a radical cation **6RC** was detected at 500−700 nm that decays by first-order kinetics with the lifetime of τ = 2.2 ± 0.2 μs. In addition, solvated electron was detected with very short decay time, τ < 50 ns. In the spectral region at 400−500 nm, two more transients were detected, decaying with $\tau \approx$ 5 μs and τ = 3 ± 1 ms. The short-lived one probably corresponds to the triplet excited state since it was quenched by O_2, whereas the long-lived one might correspond to **QM6**. Detection of the triplet excited state for **6** but not for **2**−**5** may be explained by influence of substituents at the anthracene positions 9 and 10. In anthracenes, the substitution significantly affects the photophysical properties by changing the energy gap between the anthracene S_1 and T_2 state leading to different intersystem crossing rates.[72] In an O_2-purged solution, the efficiency for the formation of radical cation and its decay kinetics were not

DOI: 10.1021/acs.joc.6b02735
J. Org. Chem. 2017, 82, 6006−6021

affected (in O_2-purged solution τ = 3.7 ± 0.2 μs). In the aqueous solution of **6**, the radical cation was not detected due to fast deprotonation. Instead, several transients were detected at 400−600 nm, two short-lived with τ = 10−30 μs, and one long-lived with τ = 0.55 ± 0.05 ms. The transients were not affected by O_2. Thus, in O_2-purged solution at 440 nm we observed a growth with a rate constant $k = 1.0 \times 10^5$ s^{-1} (τ = 10.0 ± 0.4 μs) and transients absorbing at longer wavelengths that did not decay with first-order kinetics but had similar lifetimes (τ = 13−17 μs) to the lifetime for the growth at 440 nm (see Figure S55 in the Supporting Information). One additional transient absorbing at ∼400−500 nm was also detected whose decay took place over a much longer time scale τ = 0.60 ± 0.05 ms. To ensure that the observed transients were not from the excitation of oxygenated anthracene photoproducts, the decay kinetics were measured using a flow cell. The flow rate was increased until no changes were observed for the decays, ensuring that photoproducts were not being excited. To assign the transients, quenching studies were performed with ascorbate, ubiquitous quencher for phenoxyl radical,[73] and nucleophiles (NaN_3 and ethanolamine) that quench QMs.[25,35−37,64] The quenching study revealed that the growth at 440 nm or short-lived transient (13−17 μs) absorbing at 500−600 nm do not react with nucleophiles. On the contrary, the growth at 440 nm became faster in the presence of ascorbic acid. From the growth quenching, the rate constant was estimated at $k_q = (8 \pm 2) \times 10^7$ M^{-1} s^{-1} (see Figure S56 in the Supporting Information), which is in accord with the literature precedent for phenoxyl radical ($k_q = 6.9 \times 10^8$ M^{-1} s^{-1},[74] or the radical from tyrosine at pH 7, $k_q = 4 \times 10^8$ M^{-1} s^{-1}).[75] At high ascorbate concentration (3 mM) that completely quenched the growth at 440 nm, the decays at 500−600 nm became single-exponential, revealing that the transient absorption of the phenoxyl radical **6PhO** overlaps with an additional species with the lifetime of 13−17 μs that has a strong absorbance at 580 nm. The amplitude for this transient was not affected by the addition of ascorbate, indicating that it is not formed from the phenoxyl radical. Since this transient was observed in N_2- and O_2-purged solution, it cannot be the triplet excited state or a carbon-centered radical. It does not react with nucleophiles, so it cannot be a carbocation or **QM6**. However, H_2O was required for the formation of this transient. Since this species is not involved in the formation of QMs, further studies to assign it are not within the scope of this work. On the other hand, nucleophiles quenched the long-lived transient absorbing at 400−500 nm (Table 3). Thus, the transient with the lifetime of 0.5 ms is assigned to **QM6**. In conclusion, the quenching study undoubtedly revealed the assignment of phenoxyl radical **6PhO** that absorbs at 400−550 nm. **6PhO** decays, giving a new species absorbing at 400−500 nm that lives longer, so this reaction of **6PhO** we assign to the formation of **QM6**.

Table 3. Lifetimes of QM6 and QM7 in Aqueous Solution in the Absence of Quencher and Quenching Constants with Nucleophiles (k_q/s^{-1} M^{-1}) Obtained by LFP[a]

		k_q (s^{-1} M^{-1})	
	τ (μs)	NaN_3	$HOCH_2CH_2NH_2$
QM6	550 ± 50	(8 ± 3) × 10^5	(4.8 ± 0.7) × 10^3
QM7	400 ± 50	(4.8 ± 0.8) × 10^6	(5 ± 1) × 10^4

[a]Measurement performed in air-saturated CH_3CN−H_2O (1:1) in the presence of sodium phosphate buffer (pH = 7.0, c = 0.1 M). Decays were collected at 400−500 nm in the presence of nucleophiles at different concentrations (for the quenching plots see Figures S56, S57, S62, and S63 in the Supporting Information).

In an N_2-purged CH_3CN solution of **7**, a radical cation **7RC** was detected that absorbs at 500−700 nm and decays by first-order kinetics. Interestingly, **7RC** (τ = 5.5 ± 0.3 μs) has slower decay kinetics than **6RC**. In addition, at 600−700 nm solvated electron was detected (very short decay time, <50 ns in O_2-purged solution), whereas at 400−500 nm, the triplet was detected that decayed with $\tau \approx 3$ μs (assignment based on O_2 quenching). In the region of spectrum at 400−500 nm two more transients were detected, decaying with $\tau \approx 30$ μs and τ = 0.45 ± 0.05 ms. On the basis of literature precedent, the short-lived transient was assigned to the phenoxyl radical formed by deprotonation of the radical cation,[60−62] and the long-lived transient was tentatively assigned to **7QM**. In O_2-purged CH_3CN solution of **7**, the efficiency for the formation of radical cation and its decay kinetics were not affected (in O_2-purged solution τ = 6.5 ± 0.5 μs). Similarly, the lifetime of phenoxyl radical **7PhO** was the same as in the N_2-purged solution. In the aqueous solution, the radical cation was not detected due to its very fast decay by deprotonation to phenoxyl radical, but we detected several transients absorbing at 400−600 nm. Short-lived transients with lifetimes of 25 ± 5 μs did not decay with first-order kinetics, whereas the long-lived decay was fit to single exponential with the lifetime of 100 ± 10 μs. Purging the solution with O_2 did not affect the decay of these transients nor the efficiency of their formation. Thus, in O_2-purged solution the transients have lifetimes of 40 ± 10 and 200 ± 50 μs. Similar to the photochemistry of **6**, ascorbate affected short-lived transients. Upon addition of high ascorbate concentration, the decay at 500−600 nm became single-exponential, revealing that the absorption of phenoxyl radical **7PhO** overlaps with the absorption of additional transient that was not assigned. Most importantly, quenching studies revealed that the short-lived transients do not react with nucleophiles, but the long-lived transient (200 μs) does (Table 3), so it was assigned to **QM7**.

Electron-rich alkenes are specific quenchers for QMs that react in Diels−Alder reactions.[22,25] However, attempts to quench QMs by EVE failed, in accord with the preparative irradiations where chromane products were not formed. An additional problem in the quenching experiments was the fact that EVE and aqueous CH_3CN solution containing buffer were not miscible. When EVE concentration exceeded 0.05 M, the separation of aqueous and organic layer took place. Considering the lifetime of QMs in submilliseconds, the rate constant has to be >10^5 M^{-1} s^{-1} to observe the quenching. QMs react with alkenes in Diels−Alder reactions, but the kinetics is relatively slow. For example, reported rate constant for **NQM** with EVE is $k_q = 4.1 \times 10^4$ M^{-1} s^{-1}.[25] Introducing steric hindrance with adamantane significantly slows the Diels−Alder reaction. Thus, the adamantyl derivative corresponding to NQM reacts with EVE with k_q = 85 M^{-1} s^{-1}.[37]

In summary, LFP measurements allowed for the detection of several transient species. The transients observed at 690 nm were assigned to radical cations. This assignment is clearly proven by quenching with CH_3OH and H_2O where the typical nonlinear behavior by addition of proton accepting solvent was observed, as described in literature precedent.[55,62,63] The phenoxyl radicals absorbing at 480 nm were proven by nonquenching with O_2 and similar lifetimes in aqueous and nonaqueous solution. The quenching experiments for O-centered radicals are problematic since they do not have the

DOI: 10.1021/acs.joc.6b02735
J. Org. Chem. 2017, 82, 6006−6021

same reactivity as C-centered reactive radicals. Thus, quenching with ubiquitous radical quenchers such as thiols would not be successful. The assignment of the transient to phenoxyl radical was further supported by the quenching with ascorbate. The main point of this paper is the formation of QMs. The most simple and straightforward experiment to show the existence of QMs is trapping by CH_3OH which has been conducted with success. In addition, the QM transients were quenched with two nucleophiles, ethanolamine and NaN_3, where the quenching constants undoubtedly indicated that the assignment was correct. The fact that also supports this assignment is nonquenching by O_2. Transients detected by LFP from all anthrol derivatives are compiled in Table 4.

Table 4. Transients Detected by LFP

transient	λ_{max} (nm)	lifetime
2RC	690	2.4 μs[a]
2PhO	400−550	10 μs[b]
2QM	400−500	200−300 ms[c]
3RC	690	950 ns
3OMeRC	690	3.6 μs[a]
		50 μs[b]
3PhO	300−500	10 μs[a]
3$^+$	450	0.4 s[c]
3QM	500−600	360 ns[c]
4PhO	400−550	10 μs[b]
6RC	500−700	2.2 μs[a]
6 triplet	400−500	5 μs[d]
6PhO	400−550	10 μs[b]
6QM	400−500	3 ms[a]
		0.6 ms[b]
7RC	500−700	5.5 μs[a]
7 triplet		3 μs[d]
7PhO	400−550	20−40 μs[b]
7QM	400−500	0.45 ms[a]
		200 μs[b]

[a]Detected in O_2-purged CH_3CN. [b]Detected in O_2-purged CH_3CN−H_2O (1:1). [c]Detected in O_2-purged HFIP. [d]Detected in N_2-purged CH_3CN (quenched by O_2).

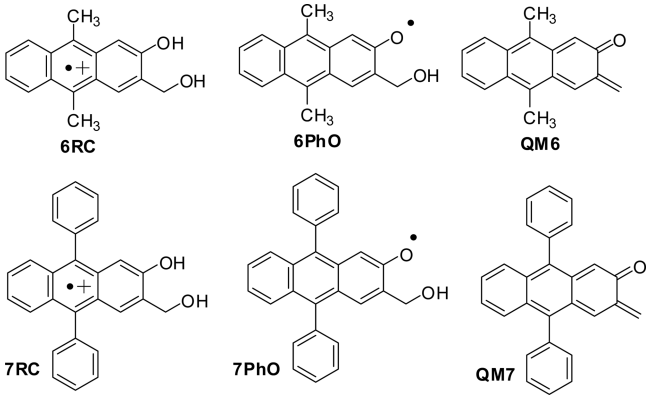

Antiproliferative Tests. The experiments were carried out on three human cell lines which are derived from three cancer types: H460 (lung carcinoma), MCF-7 (breast carcinoma), and HCT 116 (colon carcinoma). The cells were treated with the compounds in different concentration ranges and were irradiated or kept in the dark. The irradiations were performed at 350 nm (3 × 5 min) or 420 nm (3 × 15 min) 4 h after the addition of the compounds and subsequently 24 and 48 h after the first irradiation. After 72 h of incubation with the compounds, or 24 h after the last irradiation, the cell growth rate was evaluated by performing the MTT assay. A control experiment was also performed where the cells were irradiated without compounds, and the effect of irradiation was accounted for in the calculation of growth inhibition GI_{50} (Table 5, for the calculation of GI_{50} and plots of dose−responses for each compound see the Supporting Information, Figures S65 and S66). As a positive control, a psoralen derivative was used that is known to induce cytotoxic effects on exposure to irradiation due to photoinitiated DNA cross-linking.[27] Particularly important is the fact that cells could be irradiated at 420 nm, which was shown to be completely harmless for the cells in the absence of the added compounds. On the contrary, irradiation at 350 nm reduced the cell number ∼10−20%.

Antiproliferative results indicate that all compounds except **4** exhibit antiproliferative effect in the dark. Moreover, for all compounds the effect is enhanced up to 10 times upon exposure of the cells to irradiation, except for compound **5**, for which this effect was less prominent. However, with current biological data, no clear trend on the structure−activity relationship can be discerned, except that it is important to design molecules that undergo efficient photoelimination of H_2O or amine. Moreover, it is important to have chromophoric systems that can be excited with visible light that is harmless to the cells. The lack of clear structure−activity relationship may be due to different cellular accumulation of the molecules.

DISCUSSION

Understanding the mechanisms for the photogeneration of QMs is important for the rational design of molecules with desirable biological effects. To date, formation of QMs in photodehydration has always been considered to be coupled to ESIPT between phenolic OH and *o*-benzyl alcohol. Detection of two phenol conformers in S_1 with different lifetimes due to ESIPT is in agreement with such a mechanistic scheme where ESIPT gives zwitterionic phenolate in S_1 that undergoes dehydration. Moreover, our LFP data for anthrols **2**, **3**, **6**, and **7** indicate that formation of QMs from these systems can also take place via a different pathway that involves radical cations **RC** and phenoxyl radicals **PhO** (Scheme 8).

In aqueous solvent, photoionization to **RC** most probably takes place first, followed by deprotonation to phenoxyl radicals. However, in aprotic solvent, formation of phenoxyl radical may take place via H$^\bullet$ transfer (to solvent or anthrol molecule), also giving **PhO** as intermediate. Hence, formation of **PhO** by deprotonation of **RC** could not be time-resolved. Particularly surprising was the finding that decay kinetics of **PhO** matches with the QM formation kinetics. Therefore, we postulate that QMs are formed via homolytic cleavage of OH group from **PhO**, a hitherto undiscovered pathway. This photochemical process is more efficient in aqueous solution than in CH_3CN, as indicated by the more intense signal of the transient absorptions corresponding to **PhO** and QM for optically matched solutions (see Figure S35 in the Supporting Information). However, we cannot rule out formation of QMs in aprotic solvent since we see formation of weak transients in neat CH_3CN that may be assigned to QMs. Furthermore, in both protic and aprotic solvent QMs can in principle be formed through a direct photodehydration process, probably taking place via ESIPT, as well as via radical cations and phenoxyl radicals. Since anthrols can in principle be found in the aqueous

DOI: 10.1021/acs.joc.6b02735
J. Org. Chem. 2017, 82, 6006−6021

Table 5. GI_{50} (μM)[a]

cell type	conditions	2	3	4	5	psoralen[b]
HCT116	not irradiated	23 ± 4	24 ± 11	>100	17 ± 1	39 ± 24
	350 nm, 3 × 5 min	2.0 ± 0.5	8 ± 6	48 ± 12	19 ± 1	<0.01
	420 nm, 3 × 15 min	1.0 ± 0.1	3 ± 1	16 ± 2	11 ± 2	
MCF-7	not irradiated	23 ± 1	9 ± 7	>100	28.0 ± 0.7	3 ± 1
	350 nm, 3 × 5 min	2.0 ± 0.6	5 ± 2	23 ± 2	20 ± 6	0.02
	420 nm, 3 × 15 min	2.00 ± 0.01	8 ± 5	12 ± 5	9 ± 7	
H 460	not irradiated	27 ± 8	19 ± 8	>100	≥100	≥100
	350 nm, 3 × 5 min	10.0 ± 0.1	8 ± 4	≥100	31 ± 15	<0.01
	420 nm, 3 × 15 min	2.0 ± 0.5	5 ± 3	18 ± 5	12 ± 2	

[a]Concentration that causes 50% inhibition of the cell growth. The quoted errors correspond to standard deviations from at least three measurements. [b]IUPAC name: 2,5,9-trimethyl-7*H*-furo[3,2]chromen-7-one.

Scheme 8

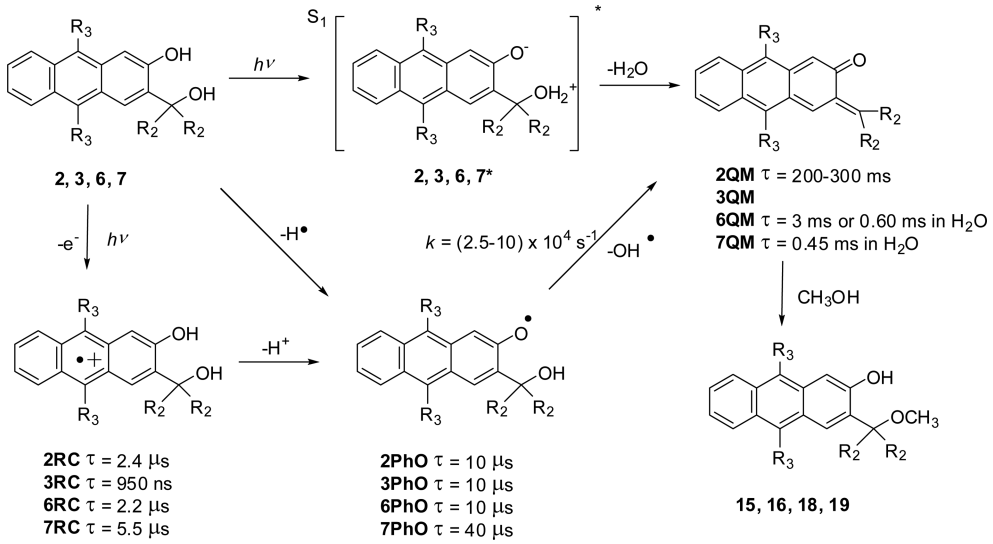

media in cytosol, or bound in the lipophilic pockets in proteins, one important aspect is to understand the role of protic media in the mechanism for the QM formation.

Adamantyl derivative **3** differs from other investigated anthrols by the highest photomethanolysis Φ_R. However, photophysical properties of **1**−**3** are very similar clearly indicating that substituents at the *o*-benzyl group do not affect reactivity in S_1 but probably affect subsequent steps that follow in S_0 after formation of primary intermediates. Thus, adamantyl and phenyl substitutents significantly enhance the stability of benzyl carbocation. Therefore, upon excitation of **3** in acidic, non-nucleophilic solvent HFIP, dehydration gave rise to $\mathbf{3}^+$. We detected carbocation $\mathbf{1}^+$ in TFE formed by protonation of the corresponding **QM1**.[33] Similarly, the dehydration to $\mathbf{3}^+$ may take place via ESPT and **QM3** or directly via heterolytic cleavage (Scheme 9). Since we could not time resolve the formation of $\mathbf{3}^+$, direct heterolysis is the most probable pathway.

Anthrols **4** and **5** are very different from the investigated series in that they undergo photodeamination. Moreover, their photophysical properties are different from alcohols **2** and **3**, indicating different reactivity in S_1 of alcohols and amines. Thus, **4** in neat CH_3CN has very low Φ_F and exhibits dual fluorescence due to equilibrium of **4** and **4zw** in S_0, as well as due to ESIPT. In aqueous solution the amine is protonated, so **4** and **5** have the same photophysical properties and reactivity. Although we were not able to detect **QM4** formed in

Scheme 9

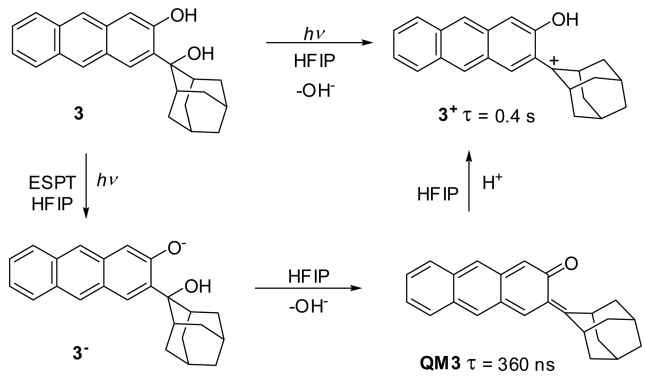

deamination from **4** and **5**, relatively high methanolysis Φ_R suggests that QM should be formed. Amine anthrol derivatives **4** and **5** were also interesting in biological context where they showed very weak cytotoxicity in the absence of irradiation (contrary to **2** and **3**) and enhancement of the antiproliferative effect on exposure of cells to irradiation.

CONCLUSIONS

We synthesized new anthrol derivatives **2**−**7** and demonstrated that they undergo photodehydration or photodeamination to form the corresponding QMs. Photodehydration may take place via ESIPT (or ESPT) that is coupled to dehydration or

DOI: 10.1021/acs.joc.6b02735
J. Org. Chem. 2017, 82, 6006−6021

via a new pathway that involves photoionization and deprotonation of the radical cation, followed by homolytic cleavage of the alcohol OH group from the phenoxyl radical. QMs were detected by LFP, and for **QM6** and **QM7** their reactivity with nucleophiles was investigated. Photodeamination in anthrol series takes place with similar efficiency as photodehydration and probably also delivers QMs. Biological investigation of anthrol molecules indicate that irradiation of cells with visible light enhances the antiproliferative effect. However, molecular structure and activity cannot be correlated. Nevertheless, high photoelimination (H_2O or amine) quantum efficiency is important for the strong enhancement of the antiproliferative effect. The most important property of the anthrols **2**–**7** is that they can be excited with light at $\lambda > 400$ nm and have high fluorescent quantum yields and relatively high quantum yields for the QM formation, rendering them suitable for different biological assays.

EXPERIMENTAL SECTION

General Information. ^{1}H and ^{13}C NMR spectra were recorded at 300 or 600 MHz at rt using TMS as a reference, and chemical shifts are reported in ppm. Melting points were determined using an Mikroheiztisch apparatus and were not corrected. IR spectra were recorded on a spectrophotometer in KBr, and the characteristic peak values are reported in cm^{-1}. HRMS were obtained on a MALDI TOF/TOF instrument. For the sample analysis, HPLC was used with a C18 (1.8 μm, 4.6 × 50 mm) column. HPLC runs were conducted at rt (~25 °C), and chromatograms were recorded using a UV detector at 254 nm. For the chromatographic separations, silica gel (0.05–0.2 mm) was used. Irradiation experiments were performed in a reactor equipped with 11 lamps with the output at 350 nm or a reactor equipped with eight lamps (1 lamp 8W). During the irradiations, the irradiated solutions were continuously purged with Ar and cooled by a tap water finger-condenser. Solvents for irradiations were of HPLC purity. Chemicals were purchased from the usual commercial sources and were used as received. Solvents for chromatographic separations were used as delivered from the suppliers (p.a. grade) or purified by distillation (CH_2Cl_2). Diethyl ether and THF used for the reaction with organolithiums was previously refluxed over Na and freshly distilled. Dry benzene was obtained after standing of commercial solvent (p.a. grade) over Na for a few days. Dry and pure acetone was obtained after a few hours of reflux of commercial acetone with $KMnO_4$ (until the violet color persisted), dried over anhydrous K_2CO_3, and finally distilled in dry atmosphere. Distilled acetone was stored over molecular sieves (4 Å). Ethanol was dried using a Mg–ethoxide method and stored over molecular sieves (4 Å). DMSO (p.a. grade) was dried by standing over molecular sieves (4 Å) for 1 week. Dry DMF was obtained after distillation of commercial solvent (p.a. grade) and standing over molecular sieves (4 Å) for few weeks. The mixture of 3-bromo-2-hydroxyanthraquinone (**9**) and 1,3-dibromo-2-hydroxyanthraquinone (**10**) was prepared according to our previous work starting from commercially available 2-aminoanthraquinone.[33]

*3-Bromo-2-hydroxyanthracene (**11**).* Sodium borohydride (3.50 g, 52.5 mmol) was dissolved in aqueous 1 M Na_2CO_3 (120 mL), and the resulting solution was heated until boiling was achieved. 2-Propanol (15 mL) was added to suppress foaming. The mixture of 2-hydroxy-3-bromoanthraquinone (**9**) and 1,3-dibromo-2-hydroxyanthraquinone (10 g, n/n = 1:1, calcd 4.4 g (15 mmol) of **9** + 5.6 g (15 mmol) of **10**, the total amount of anthraquinone was 30 mmol) was dissolved in 1 M Na_2CO_3 (120 mL) and slowly poured to the boiling solution of $NaBH_4$. Heating was continued for 15 min, with strong stirring to break the foam. To prevent formation of 2-anthrol, the reaction was quenched after 15 min by addition of 3 M HCl (100 mL), followed by the formation of a light precipitate. The solid was separated by filtration, washed with water until neutral, and dried in evacuated desiccator over KOH afford **11** (7.73 g, 95%, purity about 90%).[33]

*3-Hydroxyanthracene-2-carbaldehyde (**12**).* A flask was charged with a suspension of **11** (680 mg, 2.51 mmol) in dry Et_2O (15 mL), flushed with nitrogen, and cooled to −15 °C (ice–methanol bath). Then, 2.5 M BuLi in hexane (4.4 mL, 11 mmol) was added dropwise during 15 min, whereupon all the solid was dissolved and the solution was clear brown. The cooling bath was removed, and the reaction mixture was allowed to warm to rt during 30 min. The reaction mixture was again cooled to −15 °C, and dry DMF (1.5 mL, 19.4 mmol) was added within 5 s. Stirring was continued 1 h at −15 °C and then at rt overnight. The reaction was quenched by a careful addition of satd aq NH_4Cl (10 mL) and transferred to an extraction funnel. Three extractions with ethyl acetate were conducted (each 30 mL), the combined extracts were dried over anhydrous $MgSO_4$ and filtered, and the solvent was removed on a rotary evaporator. The crude product (brown-orange solid) was purified by chromatography on silica gel with CH_2Cl_2 as an eluent to afford aldehyde **12** (468 mg, 84%) in the form of thin bright orange crystals: 468 mg (84%); mp 222–227 °C (lit.[76,77] mp 222–232 °C); ^{1}H NMR ($CDCl_3$, 300 MHz) δ 10.13 (s, 1H), 10.07 (s, 1H), 8.53 (s, 1H), 8.40 (s, 1H), 8.25 (s, 1H), 8.00–7.92 (m, 2H), 7.52–7.40 (m, 2H), 7.39 (s, 1H); ^{13}C NMR ($CDCl_3$, 75 MHz) δ 196.4 (d), 153.7 (s), 140.6 (d), 134.5 (s), 134.4 (s), 130.5 (s), 129.4 (d), 128.6 (d), 127.6 (d), 127.4 (d), 126.4 (s), 125.1 (d), 124.1 (d), 123.7 (s), 109.9 (d); IR (KBr) ν_{max}/cm^{-1} 3285 (OH phenol), 3051 (Ar CH), 2871(CH ald), 1682 (C=O), 1452 (Ar C=C), 1167 (CO).

General Procedure for Preparation of 3-Hydroxymethyl Derivatives of 2-Anthrol. Suspension of 3-bromo-2-hydroxyanthracene (**11**) (1 equiv) in dry Et_2O was transferred to a flask and cooled to −15 °C (ice/methanol bath) in inert and dry atmosphere (N_2 balloon). BuLi (2.5 M in hexanes, 4.4 equiv) was then added dropwise during a period of 15 min. The orange suspension became clear brown until the end of BuLi addition. Then the reaction mixture was allowed to warm to rt (30 min) and again cooled to −15 °C. The solution of carbonyl compound (4.4 equiv) in dry Et_2O was added dropwise during a period of 15 min, whereas the color of reaction mixture became brighter and precipitate was formed. Stirring at −15 °C was continued for 1 h and then overnight at rt. The reaction was quenched by addition of saturated NH_4Cl solution (10 mL), and the product was extracted with ethyl acetate (3 × 25 mL). The combined extracts were dried on anhydrous $MgSO_4$ and filtered, and the solvent was removed by rotary evaporation. Crude product was purified by chromatography on silica gel using CH_2Cl_2 as an eluent.

*2-Hydroxy-3-(1-hydroxy-1-methylethyl)anthracene (**2**).* Synthesis was carried out according to the general procedure described above. Compound **11** (286 mg, 1 mmol) in dry Et_2O (10 mL), BuLi (2.5 M in hexanes, 1.2 mL, 3 mmol), and freshly distilled dry acetone (0.5 mL, 6.8 mmol) were added. The product was purified by chromatography on silica gel using CH_2Cl_2 as an eluent to afford 141 mg (56%) of pure product **2** in the form of a pale orange solid: 141 mg (56%); mp 167–168 °C; ^{1}H NMR (600 MHz, DMSO-d_6) δ 10.2 (br s, 1H), 8.42 (s, 1H), 8.22 (s, 1H), 8.07 (s, 1H), 7.98 (d, 1H, J = 8.3 Hz), 7.94 (d, 1H, J = 8.3 Hz), 7.43–7.35 (m, 2H), 7.25 (s, 1H), 5.79 (br s, 1H), 1.66 (s, 6H); ^{13}C NMR (150 MHz, DMSO-d_6) δ 153.7 (s), 138.6 (s), 132.0 (s), 131.4 (s), 129.5 (s), 128.0 (d), 127.3 (d), 127.2 (s), 125.9 (d), 125.1 (d), 124.6 (d), 123.9 (d), 121.9 (d), 107.8 (d), 72.2 (s), 29.7 (q); IR (KBr) ν_{max}/cm^{-1} 3398 (s), 2976 (m), 1647 (m), 1458 (s), 1366 (m), 1175 (s), 907 (s), 746 (s), 474 (m); HRMS-MALDI calcd for $C_{17}H_{16}O_2$ ($-e^-$) 252.1141, found 252.1144.

*2-Hydroxy-3-(2-hydroxy-2-adamantyl)anthracene (**3**).* Synthesis was carried out according to the general procedure described above. Compound **11** (250 mg, 0.92 mmol) in dry Et_2O (8 mL), BuLi (2.5 M in hexanes, 1.1 mL, 2.77 mmol), and 2-adamantanone (416 mg, 2.77 mmol) in dry Et_2O (4 mL) were added. The product was purified by chromatography on silica gel using CH_2Cl_2/hexane (2:1 → 1:0) as an eluent to afford 219 mg (69%) of product **3** in the form of yellow solid: 219 mg (69%); mp 211–213 °C; ^{1}H NMR (300 MHz, DMSO-d_6) δ 9.89 (br s, 1H), 8.49 (s, 1H), 8.22 (s, 1H), 8.04 (s, 1H), 7.96 (t, 2H, J = 7.7 Hz), 7.46–7.33 (m, 2H), 7.28 (s, 1H), 5.15 (br s, 1H), 2.80 (br s, 2H), 2.52 (s, 1H), 2.39 (s, 1H), 2.08–1.73 (m, 6H), 1.71 (s, 2H), 2.20 (s, 1H), 1.00 (s, 1H); ^{13}C NMR (75 MHz, DMSO-d_6) δ 154.7 (d), 135.2 (d), 131.61 (d), 131.58 (d), 129.5 (d), 128.0 (s), 127.3 (s), 127.1 (d), 127.0 (d), 126.3 (s), 125.3 (s), 123.9 (s), 121.8

DOI: 10.1021/acs.joc.6b02735
J. Org. Chem. 2017, 82, 6006–6021

(s), 108.5 (s), 75.9 (s), 46.3 (s), 38.4 (d), 37.6 (d), 35.5 (d), 34.9 (d), 34.8 (s), 32.7 (d), 26.8 (s), 26.4 (s); IR (KBr) ν_{max}/cm^{-1} 3332 (m), 2907 (vs), 2856 (s), 1718 (s), 1452 (m), 1283 (m), 904 (s), 744 (s), 471 (m); HRMS-MALDI calcd for $C_{24}H_{24}O_2$ ($-OH^-$) 327.1743, found 327.1743.

*3-(2-Hydroxyadamantantan-2-yl)-2-methoxyanthracene (**3OMe**).* Compound **3** (20 mg, 0.058 mmol) was dissolved in acetone (10 mL), and K_2CO_3 (138 mg, 1 mmol) was added. The resulting suspension was heated until reflux was achieved, wherein all compound was converted to salt (anthrolate), which was visible in color change from pale yellow to yellow. The reaction mixture was then cooled to rt, and MeI (50 μL, 0.8 mmol) was added. Stirring at rt was continued for 5 h, during which time the color changed back to pale yellow, which indicated completion of the reaction (confirmed by TLC analysis). The reaction mixture was filtered, and the solvent was removed on a rotary evaporator. The crude product was purified by chromatography on silica gel using CH_2Cl_2–hexane (1:1 → 1:0) as an eluent to afford 18 mg (86%) of product **3OMe** in the form of a pale yellow solid: 18 mg (86%); mp 233–234 °C; ^{1}H NMR (300 MHz, $CDCl_3$) δ 8.34 (s, 1H), 8.22 (s, 1H), 8.02 (s, 1H), 7.99–7.89 (m, 2H), 7.48–7.37 (m, 2H), 7.25 (s, 1H), 4.00 (s, 3H), 2.81 (s, 2H), 2.62 (s, 1H), 2.59 (s, 2H), 2.03–1.64 (m, 10H); ^{13}C NMR (150 MHz, $CDCl_3$) δ 156.3 (s), 134.9 (s), 132.1 (s), 131.3 (s), 130.5 (s), 128.1 (d), 127.9 (d), 127.7 (s), 127.4 (d), 126.4 (d), 125.3 (d), 124.3 (d), 123.3 (d), 104.8 (d), 76.8 (s), 55.0 (q), 37.9 (t), 35.5 (d), 35.3 (t), 33.1 (t), 27.3 (d), 26.9 (d); IR (KBr) ν_{max}/cm^{-1} 3558 (m), 2887 (m), 1629 (m), 1429 (m), 1213 (s), 1005 (m), 922 (m), 746 (m) 586 (w), 471 (m); HRMS-MALDI calcd for $C_{25}H_{26}O_2$ ($-e^-$) 358.1927, found 358.1916.

*3-[(Diethylamino)methyl]-2-hydroxyanthracene (**4**).* Aldehyde **12** (120 mg, 0.54 mmol) was suspended in a solution of Et_2NH (φ = 35%) in dry ethanol ($V_{solution}$ = 10 mL). The suspension was stirred for 16 h at rt under N_2 inert atmosphere. $NaBH_4$ (100 mg, 2.64 mmol) was added whereupon intensive foaming occurred, finally resulting in clear solution. Stirring was continued for 4 h at rt, and then volatile constituents (EtOH, excess of Et_2NH) were evaporated on a rotary evaporator (protected from light). Water (50 mL) was added to dissolve inorganic salts, and the product was extracted with CH_2Cl_2 (4 × 25 mL). The combined organic extracts were dried over anhydrous Na_2SO_4 and filtered, and the solvent was removed on a rotary evaporator to afford 139 mg (93%) of amine **4** in the form of an orange solid: 139 mg (93%); mp >300 °C dec; ^{1}H NMR (300 MHz, $CDCl_3$) δ 8.25 (s, 1H), 8.20 (s, 1H), 7.90 (d, 2H, J = 9.3 Hz), 7.67 (s, 1H), 7.42–7.33 (m, 2H), 7.29 (s, 1H), 4.22 (s, 2H), 2.80 (q, 4H, J = 7.0 Hz), 1.27 (t, 6H, J = 7.0 Hz); ^{13}C NMR (150 MHz, $CDCl_3$) δ 132.7 (s), 132.0 (s), 130.0 (s), 128.0 (d), 127.52 (d), 127.49 (s), 127.3 (d), 125.6 (d), 125.1 (d), 124.0 (d), 123.3 (d), 108.5 (d), 53.8 (t), 46.3 (t), 14.7 (q); IR (KBr) ν_{max}/cm^{-1} 3420 (m), 2957 (m), 1626 (w), 1431 (s), 897 (m), 738 (m), 469 (w); HRMS-MALDI calcd for $C_{19}H_{21}NO$ ($-e^-$) 279.1618, found 279.1612.

*3-[(Diethylamino)methyl]-2-hydroxyanthracene hydrochloride (**5**).* Because of the poor solubility of the amine **4** in Et_2O, the precipitation was conducted in CH_2Cl_2. Amine **4** (15 mg, 0.05 mmol) was dissolved in CH_2Cl_2 (2 mL), and a solution of HCl in Et_2O was added until complete precipitation occurred. An additional volume of Et_2O (5 mL) was added to complete the precipitation. The solution was decanted, and the precipitate was washed with Et_2O (3 × 2 mL) and then dried in vacuum to obtain 12 mg (71%) of product **5** in the form of a light gray-brown powder: 12 mg (71%); mp >300 °C dec; ^{1}H NMR (300 MHz, DMSO-d_6) δ 8.48 (s, 1H), 8.33 (s, 1H), 8.17 (s, 1H), 8.08–7.95 (m, 2H), 7.52–7.40 (m, 2H), 7.39 (s, 1H), 4.28 (s, 2H), 2.95–2.86 (q, 4H, J = 7.2 Hz), 1.18 (t, 6H, J = 7.2 Hz); ^{13}C NMR (75 MHz, DMSO-d_6) δ 153.5 (s), 133.11 (s), 133.08 (s), 131.8 (d), 130.1 (s), 128.7 (d), 127.9 (d), 127.1 (s), 126.8 (d), 126.3 (d), 124.9 (d), 123.8 (s), 123.3 (d), 107.3 (d), 55.5 (t), 45.7 (t), 11.3 (q); IR (KBr) ν_{max}/cm^{-1} 3407 (s), 2953 (s), 1637 (s), 1446 (s), 1208 (m), 1129 (m), 744 (m), 471 (m); HRMS-MALDI calcd for $C_{19}H_{21}NO$ ($-e^-$) 279.1618, found 279.1619.

*3-Bromo-9,10-dimethyl-2-hydroxyanthracene (**13-Me**).* Bromoanthraquinone **9** (1.4 g, 4.64 mmol) was placed in a flask and dissolved in dry THF (50 mL) under inert atmosphere (N_2 balloon). The resulting solution was cooled to 0 °C (ice bath), and 1.1 M MeLi in Et_2O (14.6 mL, 16 mmol) was added dropwise over a period of 15 min. The reaction mixture was stirred at rt for 1 h and then quenched by a careful addition of satd aq NH_4Cl (20 mL). Water (300 mL) was added, and the resulting suspension was extracted with Et_2O (3 × 20 mL). The combined organic extracts were dried over anhydrous $MgSO_4$ and filtered, and the solvent was removed on a rotary evaporator to give the crude diol product, which was immediately used in the next step.

A flask (250 mL) was charged with Et_2O (40 mL), and $SnCl_2$ (7.74 g, 40.8 mmol) was added carefully. Concentrated HCl (8 mL) was added portionwise, causing release of heat and extensive foaming. After the mixture was cooled to rt, the solution of crude diol product in THF (5 mL) was added (at once), and stirring was continued for 20 min. The reaction was quenched by addition of water (100 mL), and the product was extracted with Et_2O (3 × 25 mL). The combined organic extracts were dried over anhydrous $MgSO_4$ and filtered, and the solvent was removed on a rotary evaporator to give the crude product (3 g) which was purified by chromatography on silica gel using CH_2Cl_2 as an eluent to afford the pure product **13-Me** (1.00 g, 72%) in the form of yellow-brown solid: 1.00 g (72%); mp 130–132 °C; ^{1}H NMR (300 MHz, $CDCl_3$) δ 8.49 (s, 1H), 8.28–8.18 (m, 2H), 7.77 (s, 1H), 7.53–7.39 (m, 2H), 5.62 (s, 1H), 2.98 (s, 3H), 2.96 (s, 3H); ^{13}C NMR (75 MHz, $CDCl_3$) δ 147.9 (s), 130.4 (s), 130.2 (s), 129.0 (d), 128.9 (s), 127.7 (s), 126.9 (s), 126.5 (s), 125.24 (d), 125.15 (d), 124.9 (d), 124.3 (d), 113.5 (s), 106.9 (d), 14.18 (q), 14.13 (q); IR (KBr) ν_{max}/cm^{-1} 3448 (s), 1672 (s), 1578 (m), 1443 (w), 1335 (m), 1024 (w), 754 (m); HRMS (MALDI) calcd for $C_{16}H_{13}BrO$ ($-e^-$) 300.0150, found 300.0150.

*9,10-Dimethyl-2-hydroxyanthracene-3-carbaldehyde (**14-Me**).* A flask (250 mL) was charged with bromide **13-Me** (984 mg, 3.27 mmol), and dry Et_2O (40 mL) was added. The resulting suspension was cooled to −15 °C (ice–methanol bath) under inert atmosphere (N_2). Then, 2.5 M BuLi in hexane (4 mL, 9.8 mmol) was added dropwise. The stirring was continued 10 min at −15 °C and then 30 min at rt. The reaction mixture was again cooled to −15 °C, and dry DMF (1 mL, 13 mmol) was added (at once), causing the formation of a yellow precipitate. The stirring was continued 10 min at −15 °C and 2 h at rt. The reaction was quenched by a careful addition of 1 M HCl (100 mL) with vigorous stirring until the yellow color completely turned to red. The product was extracted with CH_2Cl_2 (3 × 25 mL). The combined extracts were dried over anhydrous $MgSO_4$ and filtered, and the solvent was removed on a rotary evaporator. The crude product was crystallized from CH_2Cl_2-Et_2O (3:2) to afford the pure product **14-Me** (818 mg, 75%) in the form of dark red crystalline solid: 818 mg (75%); mp 169–170 °C; ^{1}H NMR (300 MHz, $CDCl_3$) δ 10.07 (s, 1H), 9.99 (s, 1H), 8.55 (s, 1H), 8.27–8.13 (m, 2H), 7.57 (s, 1H), 7.56–7.41 (m, 2H), 3.05 (s, 3H), 2.90 (s, 3H); ^{13}C NMR (75 MHz, $CDCl_3$) δ 196.5 (d), 152.9 (s), 137.7 (d), 131.8 (s), 132.6 (s), 132.1 (s), 128.7 (s), 126.7 (d), 126.3 (s), 125.6 (d), 124.9 (d), 124.8 (s), 124.4 (d), 122.5 (s), 107.7 (d), 14.22 (q), 14.16 (q); IR (KBr) ν_{max}/cm^{-1} 3209 (w), 3076 (w), 2926 (w), 2847 (w), 1655 (s), 1389 (m), 1190 (m), 746 (w), 579 (w); HRMS (MALDI) calcd for $C_{17}H_{14}O_2$ ($-e^-$) 250.0994, found 250.0988.

*9,10-Dimethyl-2-hydroxy-3-hydroxymethylanthracene (**6**).* Aldehyde **14-Me** (400 mg, 1.6 mmol) was dissolved in THF (25 mL) and water was added (25 mL), followed by the addition of $NaBH_4$ (180 mg, 4.8 mmol). The resulting mixture was stirred at rt protected from light for 1 h. The reaction was quenched by addition of 0.2 M HCl (30 mL). Water was added (200 mL), the suspension was stirred for additional 30 min, then the product was collected by filtration. The crude product was washed thoroughly with water and then dried in evacuated desiccator over KOH overnight to afford the pure product **6** (352 mg, 87%) in the form of a yellowish powder: 352 mg (87%); mp 179–181 °C; ^{1}H NMR (300 MHz, DMSO-d_6) δ 9.98 (s, 1H), 8.32–8.20 (m, 3H), 7.51–7.39 (m, 3H), 5.27 (t, 1H, J = 5.3 Hz), 4.71 (d, 2H, J = 5.3 Hz), 3.01 (s, 3H), 2.89 (s, 3H); ^{13}C NMR (75 MHz, DMSO-d_6) δ 152.7 (s), 132.4 (s), 130.3 (s), 129.4 (s), 127.7 (s), 127.4 (s), 125.4 (s), 125.3 (d), 124.65 (d), 124.58 (d), 124.0 (s), 123.5 (d),

DOI: 10.1021/acs.joc.6b02735
J. Org. Chem. 2017, 82, 6006–6021

122.6 (d), 103.9 (d), 58.9 (t), 13.9 (q, 2C); IR (KBr) ν_{max}/cm^{-1} 3518 (s), 3155 (s), 2936 (w), 1637 (s), 1184 (m), 980 (m), 743 (m); HRMS (MALDI) calcd for $C_{17}H_{16}O_2$ ($-e^-$) 252.1150, found 252.1147.

*3-Bromo-9,10-diphenyl-2-hydroxyanthracene (**13-Ph**).* Bromoanthraquinone **9** (303 mg, 1 mmol) was placed in a flask (100 mL), and dry benzene (20 mL) was added. The resulting solution was cooled to 0 °C (ice bath) under inert and dry atmosphere (N_2), and 1.9 M PhLi in *n*-Bu_2O (7.5 mL, mmol) was added dropwise. The stirring was continued for 1 h at 0 °C and then at rt overnight. The reaction was quenched by a careful addition of water (10 mL) followed by the addition of 1 M HCl (100 mL). The product was extracted with ether (3 × 25 mL), the combined extracts were dried over anhydrous $MgSO_4$ and filtered, and the solvent was removed on a rotary evaporator. Then ether was added (20 mL), and the resulting solution was heated to reflux on a hot water bath. Concentrated HI (4 mL) was added dropwise during 5 min under inert atmosphere (N_2). Reflux was continued for 20 min. The cooled reaction mixture was transferred to an extraction funnel, ether (30 mL) was added, and the organic phase was washed with 5% Na_2SO_3 (25 mL) and water (3 × 50 mL). The ethereal phase was separated, dried over anhydrous $MgSO_4$, and filtered, and the solvent was removed on a rotary evaporator. The product was purified by chromatography on silica gel using CH_2Cl_2 as an eluent to give the pure product **13-Ph** (293 mg, 69%) in the form of yellow-brown powder: 293 mg (69%); mp 259–260 °C; ^{1}H NMR (300 MHz, DMSO-d_6) δ 10.60 (s, 1H), 7.76–7.55 (m, 7H), 7.52–7.41 (m, 6H), 7.40–7.28 (m, 2H), 7.05 (s, 1H); ^{13}C NMR (75 MHz, DMSO-d_6) δ 150.8 (s), 138.3 (s), 137.8 (s), 135.7 (s), 133.8 (s), 130.85 (d), 130.79 (d), 130.2 (d), 129.9 (s), 129.8 (s), 128.8 (d), 128.7 (d), 127.95 (d), 127.88 (s), 126.4 (d), 125.8 (d), 125.7 (d), 124.6 (d), 114.8 (s), 106.9 (d); IR (KBr) ν_{max}/cm^{-1} 3446 (s), 2917 (m), 2848 (m), 1634 (m), 691 (w); HRMS (MALDI) calcd for $C_{26}H_{17}BrO$ ($-e^-$) 424.0463, found 424.0463.

*9,10-Diphenyl-2-hydroxyanthracene-3-carbaldehyde (**14-Ph**).* In a flask (100 mL), bromide **13-Ph** (430 mg, 1 mmol) was dissolved in dry Et_2O (20 mL) and the solution cooled to −15 °C (ice–methanol bath) under inert and dry atmosphere (N_2). A 2.5 M solution of BuLi in hexane (1.2 mL, 3 mmol) was added dropwise over a period of 5 min. Stirring was continued for 5 min at −15 °C and then 30 min at rt, and the solution was finally again cooled to −15 °C. Dry DMF (1 mL, 13 mmol) was added (at once), causing forming of a yellow precipitate. Stirring was continued for 30 min at −15 °C and then 1 h at rt. The reaction was quenched by careful addition of 0.5 M HCl (100 mL) with vigorous stirring until all yellow solid turned to red. The product was extracted with Et_2O (3 × 35 mL), the combined extracts were dried over anhydrous $MgSO_4$ and filtered, and the solvent was removed on a rotary evaporator. The product was purified by chromatography on silica gel using CH_2Cl_2 as an eluent to give the pure product **14-Ph** (300 mg, 80%) in the form of red crystalline solid: 300 mg (80%); mp 211–212 °C; ^{1}H NMR (600 MHz, $CDCl_3$) δ 9.97 (s, 1H), 9.89 (s, 1H), 8.11 (s, 1H), 7.67–7.57 (m, 7H), 7.55–7.52 (m, 1H), 7.51–7.47 (m, 2H), 7.44–7.41 (m, 2H), 7.38 (m, 1H), 7.31–7.27 (m, 1H), 7.09 (s, 1H); ^{13}C NMR (150 MHz, $CDCl_3$) δ 196.7 (d), 153.2 (s), 140.4 (s), 139.7 (d), 138.3 (s), 137.8 (s), 135.1 (s), 132.8 (s), 132.7 (s), 131.1 (d), 131.0 (d), 128.9 (s), 128.6 (d), 128.5 (d), 128.1 (d), 127.7 (d), 127.5 (d), 127.0 (d), 126.6 (d), 125.1 (s), 124.8 (d), 123.0 (s), 109.3 (d); IR (KBr) ν_{max}/cm^{-1} 3243 (w), 3058 (w), 1663 (vs), 1541 (w), 1389 (m), 1146 (m), 700 (m), 596 (w); HRMS (MALDI) calcd for $C_{27}H_{18}O_2$ ($-e^-$) 374.1307, found 374.1310.

*9,10-Diphenyl-2-hydroxy-3-(hydroxymethyl)anthracene (**7**).* Aldehyde **14-Ph** (262 mg, 0.7 mmol) was dissolved in ethanol (25 mL) and water was added (25 mL) followed by the addition of $NaBH_4$ (40 mg, 1.05 mmol). The resulting solution was protected from light and stirred at rt under inert atmosphere (N_2) overnight. The reaction was quenched by addition of 1 M HCl (20 mL) and stirred for additional 15 min, and the product was collected by filtration. The product was washed thoroughly with water and then dried in evacuated desiccator over KOH overnight to yield the product **7** (253 mg, 96%) in the form of a yellowish solid: 253 mg (96%); mp 200–201 °C; ^{1}H NMR (600 MHz, DMSO-d_6) δ 9.86 (s, 1H), 7.69–7.62 (m, 5H), 7.61–7.56 (m, 2H), 7.50–7.41 (m, 6H), 7.33–7.24 (m, 2H), 6.87 (s, 1H), 4.99 (s, 1H), 4.54 (s, 2H); ^{13}C NMR (75 MHz, DMSO-d_6) δ 152.9 (s), 139.1 (s), 138.8 (s), 136.1 (s), 133.3 (s), 133.0 (s), 130.9 (d), 130.3 (s), 129.2 (s), 128.8 (d), 128.6 (d), 127.6 (d), 127.5 (s), 127.4 (d), 126.4 (d), 125.7 (d), 125.4 (s), 124.9 (d), 123.8 (d), 123.7 (d), 104.9 (d), 58.5 (t); IR (KBr) ν_{max}/cm^{-1} 3341 (s), 3059 (w), 2918 (w), 1637 (s), 1491 (w), 1441 (s), 1240 (m), 1138 (m), 986 (w), 702 (s), 592 (w); HRMS (MALDI) calcd for $C_{27}H_{20}O_2$ ($-e^-$) 376.1463, found 376.1459.

Photochemical Experiments. *Preparative Photochemical Methanolysis.* Compound (15 mg) was dissolved in methanol (80 mL), water (20 mL) was added, and the resulting clear solution was purged with stream of Ar gas (20 min) in the glass vessel (ordinary glass). Photolysis was carried out in a reactor using 12 lamps at 350 nm. Photoreactions were monitored by HPLC (for method details and chromatograms, see the SI), and irradiations were stopped when conversion reached >80%. The solvent was removed on a rotary evaporator, and crude products were purified by chromatography on silica gel using CH_2Cl_2 as the eluent.

*2-Hydroxy-3-(1-methyl-1-methoxyethyl)anthracene (**15**).* Preparative photolysis was carried out according to the general procedure described above with irradiation for 60 min. After chromatography, product **15** (13 mg, 82%) was isolated in the form of pale yellow film on the walls of the flask: 13 mg (82%); mp 139–140 °C; ^{1}H NMR (300 MHz, $CDCl_3$) δ 8.91 (s, 1H), 8.31 (s, 1H), 8.21 (s, 1H), 7.92 (d, 2H, J = 9.1 Hz), 7.75 (s, 1H), 7.45–7.33 (m, 2H), 7.35 (s, 1H), 3.29 (s, 3H), 1.77 (s, 6H); ^{13}C NMR (75 MHz, $CDCl_3$) δ 153.6 (s), 132.63 (s), 132.57 (s), 132.3 (s), 130.2 (s), 128.1 (d), 127.6 (d), 127.5 (s), 126.5 (d), 126.2 (d), 125.4 (d), 124.2 (d), 123.2 (d), 109.5 (d), 80.2 (s), 51.1 (q), 26.5 (q); IR (KBr) ν_{max}/cm^{-1} 3455 (m), 3155 (w), 2936 (w), 2856 (w), 1655 (s), 1334 (m), 1154 (w); HRMS-MALDI calcd for $C_{18}H_{18}O_2$ ($-e^-$) 266.1310, found 266.1309.

*2-Hydroxyanthracenyl-3-(2-methoxy-2-adamantyl)anthracene (**16**).* Preparative photolysis was carried out according to the general procedure described above. Irradiated for 25 min. After chromatography, product **16** (10 mg, 64%) was isolated in the form of pale yellow film on the walls of the flask: 10 mg (64%); dec >112 °C; ^{1}H NMR (600 MHz, $CDCl_3$) δ 8.37 (s, 1H), 8.33 (s, 1H), 8.19 (s, 1H), 7.99 (s, 1H), 7.91 (t, 2H, J = 7.9 Hz), 7.42–7.34 (m, 2H), 7.35 (s, 1H), 3.10 (s, 3H), 2.80–2.75 (m, 2H), 2.58 (t, 2H, J = 13 Hz), 2.26 (d, 1H, J = 13 Hz), 2.11–2.07 (m, 1H), 1.93 (s, 1H), 1.85 (s, 1H), 1.79–1.70 (m, 3H), 1.70–1.60 (m, 2H), 1.39 (d, 1H, J = 13 Hz); ^{13}C NMR (150 MHz, $CDCl_3$) δ 153.6 (s), 132.3 (s), 130.2 (s), 130.1 (s), 129.9 (d), 128.1 (d), 127.5 (d), 127.2 (s), 126.3 (d), 125.4 (d), 124.2 (d), 123.1 (d), 110.2 (d), 84.0 (s), 48.8 (q), 37.7 (t), 36.4 (t), 35.5 (d), 34.2 (t), 33.2 (t), 32.5 (t), 30.8 (d), 27.2 (d), 26.8 (d); IR (KBr) ν_{max}/cm^{-1} 3558 (m), 2887 (s), 1630 (m), 1429 (m), 1213 (s), 1005 (m), 746 (m), 471 (m); HRMS-MALDI calculated for $C_{25}H_{26}O_2$ ($-e^-$) 358.1933, found 358.1924.

*3-Methoxymethyl-2-hydroxyanthracene (**17**).* Preparative photolysis was carried out according to the general procedure described above with irradiation for 15 min. After chromatography, product **17** (15 mg, 99%) was isolated in the form of form of pale yellow film on the walls of the flask: 15 mg (99%); mp 189–192 °C; ^{1}H NMR (300 MHz, $CDCl_3$) δ 8.29 (s, 1H), 8.22 (s, 1H), 7.95–7.88 (m, 2H), 7.73 (s, 1H), 7.45–7.37 (m, 2H), 7.36 (s, 1H), 4.84 (s, 2H), 3.50 (s, 3H); ^{13}C NMR (75 MHz, $CDCl_3$) δ 153.5 (s), 132.8 (s), 132.2 (s), 130.3 (s), 128.2 (d), 128.0 (d), 127.7 (d), 126.2 (s), 126.1 (d), 125.5 (d), 124.4 (d), 123.8 (d), 109.3 (d), 74.2 (t), 58.2 (q); IR (KBr) $\tilde{\nu}$ 3228 (m), 2928 (m), 1637 (s), 1445 (m), 1213 (m), 1076 (m), 887 (s), 737 (m), 473 (m); HRMS-MALDI calcd for $C_{16}H_{14}O_2$ ($-e^-$) 238.0990, found 238.0991.

*9,10-Dimethyl-2-hydroxy-3-(methoxymethyl)anthracene (**18**).* Preparative photolysis was carried out according to the general procedure described above with irradiation for 30 min with 10 lamps at 350 nm. After chromatography, product **18** (10 mg, 64%) was isolated in the form of pale yellow solid: 10 mg (64%); mp >171 °C dec; ^{1}H NMR (600 MHz, $CDCl_3$) δ 8.26 (t, 2H, J = 7.6 Hz), 8.06 (s, 1H), 7.68 (s, 1H), 7.58 (s, 1H), 7.51–7.42 (m, 2H), 4.92 (s, 2H), 3.53 (s, 3H), 3.05 (s, 3H), 3.00 (s, 3H); ^{13}C NMR (150 MHz, $CDCl_3$) δ

DOI: 10.1021/acs.joc.6b02735
J. Org. Chem. 2017, 82, 6006–6021

152.8 (s), 131.1 (s), 130.3 (s), 128.5 (s), 128.3 (s), 125.9 (s), 125.7 (s), 125.3 (d), 125.2 (d), 124.83 (d), 124.82 (d), 123.7 (d), 107.2 (d), 74.6 (t), 58.2 (q), 14.13 (q), 14.10 (q); IR (KBr) ν_{max}/cm^{-1} 3390 (s), 2928 (m), 1649 (s), 448 (m), 1078 (m), 754 (s); HRMS (MALDI) calcd for $C_{18}H_{18}O_2$ ($-e^-$) 266.1307, found 266.1317.

*9,10-Diphenyl-2-hydroxy3-(methoxymethyl)anthracene (**19**).* Preparative photolysis was carried out according to the general procedure described above with irradiation for 30 min with 10 lamps at 350 nm. After chromatography, product **19** (12 mg, 77%) was isolated in the form of pale yellow solid: 12 mg (77%); mp >149 °C dec; ^{1}H NMR (600 MHz, $CDCl_3$) δ 7.64−7.50 (m, 10H), 7.51 (s, 1H), 7.48−7.43 (m, 4H), 7.42 (s, 1H), 7.08 (s, 1H), 4.69 (s, 2H), 3.43 (s, 3H); ^{13}C NMR (150 MHz, DMSO-d_6) δ 139.4 (s), 139.0 (s), 138.9 (s), 137.0 (s), 134.7 (s), 131.2 (d), 131.1 (d), 131.1 (s), 130.3 (s), 128.5 (s), 128.4 (d), 128.3 (d), 127.4 (d), 127.3 (d), 126.9 (d), 126.8 (d), 126.4 (d), 125.7 (s), 125.4 (s), 125.1 (d), 124.0 (d), 108.5 (d), 74.3 (t), 58.2 (q); IR (KBr) ν_{max}/cm^{-1} 3403 (s), 3056 (w), 2920 (s), 2845 (w), 1637 (m), 1460 (m), 702 (s); HRMS (MALDI) calcd for $C_{28}H_{22}O_2$ ($-e^-$) 390.1620, found 390.1609.

Irradiations in the Presence of Different Concentrations of Water. Solutions of anthrols (**2**, **3**, **4**, and **5**, $c = 3 \times 10^{-4}$ M) were prepared in CH_3OH to which a fraction of H_2O was added (0, 5, 10, and 20% v/v). The solutions were purged with a stream of N_2 (20 min) and then sealed with a septum. The test tubes were irradiated at the same time in a reactor with eight lamps with an output at 350 nm, and the samples were taken at the given time and analyzed by HPLC (for example, see Figure S1).

Quantum Yields of Methanolysis. Quantum yields for the photomethanolysis reactions were determined by using three actinometers simultaneously: valerophenone,[43,44] ferrioxalate,[43,45] and KI/KIO_3,[43,46] as recently described by us.[33] The measurement was performed in five quartz cells with the same dimensions that were irradiated from the front side only. Solutions of anthrols **2**−**7** in CH_3OH−H_2O (4:1), and actinometers were freshly prepared and their concentrations adjusted to have absorbances of 0.4−0.8 at 254 nm. After adjustment of the concentrations and measurement of the corresponding UV−vis spectra, 2.5 mL of the solutions were transferred to the quartz cells, and the solutions were purged with a stream of N_2 (20 min) and then sealed with a cap. The cells were placed in a holder, which ensured equal distance of all samples from the lamp and were irradiated at the same time in the reactor with 1 lamp at 254 nm for 30 s. Before and after the irradiation, the samples were taken from the cells by use of a syringe and analyzed by HPLC to determine photochemical conversions. The conversion did not exceed 30% to avoid a change of the absorbance or filtering of the light by the product. From the conversion of actinometers irradiance was calculated. Similar values were obtained for all three actinometers. The mean value of three measurements was reported. All equations for the calculation of quantum yields are given in the Supporting Information (eqs S1−S5).

Steady-State and Time-Resolved Fluorescence Measurements. Fluorescence measurements were performed on a PTI QM40 fluorometer at 20 °C. All slits (excitation and emission) were set to the bandpass of 2 nm. The spectra were corrected for the fluctuations in lamp intensity and transmission of optics. The samples were excited at 340, 350, or 370 nm, and the emission was collected in the range of 350−670 nm (or 380−700 nm). Fluorescence quantum yields were determined by use of quinine sulfate in 1.0 N H_2SO_4 as reference (Φ_F = 0.55).[52] Fluorescence decays, collected over 1023 time channels, were obtained on an Edinburgh Instruments OB920 single-photon counter using a pulsed laser diode for excitation at 375 nm. The instrument response functions, using LUDOX as the scatterer, were recorded at the same wavelengths as the excitation wavelength and had a half width of ~0.2 ns. The time increment per channel was 0.020 ns. Emission decays were recorded until they reached 3×10^3 counts in the peak channel for anthrols **1**−**3** at 410, 430, and 450 nm (and 550 nm for the decays in aqueous solution), for **4** and **5** at 420, 450, 550, and 575 nm, and for **6** and **7** at 440, 460, and 500 nm (and 550 nm for the decays in aqueous solution). Global analysis of decays was performed by fitting to sum of exponentials using global Gaussian-weighted nonlinear least-squares fitting based on Marquardt−Levenberg minimization implemented in the Fast software package from Edinburgh Instruments. The fitting parameters (decay times and pre-exponential factors) were determined by minimizing the reduced chi-square χ^2 and graphical methods were used to judge the quality of the fit that included plots of the weighted residuals vs channel number. Decay times were kept linked for decays collected over different wavelengths. Details about fitting procedures and fits can be found in the Supporting Information (eqs S7−S13, Figures S25−S27, and Tables S1 and S2). Time-resolved emission spectra for the aqueous solution of **7** were recorded by collecting decays in the range 420−670 nm with an increment of 10 nm and with a fixed decay collection time.

Laser Flash Photolysis (LFP). All LFP studies were performed on a system previously described[78] using as an excitation source a pulsed Nd:YAG laser at 355 nm (<50 mJ per pulse) with a pulse width of 10 ns. Static cells (7 mm × 7 mm) were used, and the solutions were purged with nitrogen or oxygen for 20 min prior to performing the measurements. In some of the quenching experiments with ascorbate, the solution was flowed through a cell with the rate to ensure that each laser pulse was absorbed by a fresh solution. Absorbances at 355 nm were ~0.3−0.5. For the collection of decays at long time scales, a modification of the setup was used, wherein the probing light beam from the Xe lamp was not pulsed, as previously described.[79] However, precise determination of long-lived lifetimes was problematic since the lamp intensity fluctuated on the tenth of millisecond time scale. Measurements of **6** and **7** in CH_3CN−H_2O (1:1) were conducted in the presence of phosphate buffer (0.1 M, pH = 7.0), whereas for **2**−**5** nonbuffered H_2O was used. Addition of buffers to the solutions may drastically change photophysical properties, and photochemical reactivity since buffers react with the excited states of molecules undergoing ESPT.[53,54] To circumvent these excited state reactions with buffer, we omitted the use of buffers in some examples.

■ ASSOCIATED CONTENT

Supporting Information

The Supporting Information is available free of charge on the ACS Publications website at DOI: 10.1021/acs.joc.6b02735.

UV−vis and fluorescence spectra of **2**−**7**, LFP data, antiproliferative tests, and ^{1}H and ^{13}C NMR spectra (PDF)

■ AUTHOR INFORMATION

Corresponding Author

*E-mail: nbasaric@irb.hr. Fax: + 385 1 4680 195. Tel: +385 1 4561 141.

ORCID

Cornelia Bohne: 0000-0001-9996-0076

Nikola Basarić: 0000-0001-9412-9734

Notes

The authors declare no competing financial interest.

■ ACKNOWLEDGMENTS

These materials are based on work financed by the Croatian Foundation for Science (HRZZ IP-2014-09-6312 and IP-11-2013-5660), the Natural Sciences and Engineering Research Council of Canada (NSERC- RGPIN-121389-2012), and the University of Victoria (UVIC).

■ REFERENCES

(1) Rokita, S. E., Ed. *Quinone Methides*; Wiley: Hoboken, 2009.

(2) Li, V. S.; Kohn, H. *J. Am. Chem. Soc.* **1991**, *113*, 275−283.

(3) Han, I.; Russell, D. J.; Kohn, H. *J. Org. Chem.* **1992**, *57*, 1799−1807.

DOI: 10.1021/acs.joc.6b02735
J. Org. Chem. 2017, 82, 6006−6021

(4) Tomasz, M.; Das, A.; Tang, K. S.; Ford, M. G. J.; Minnock, A.; Musser, S. M.; Waring, M. J. *J. Am. Chem. Soc.* **1998**, *120*, 11581−11593.
(5) Freccero, M. *Mini-Rev. Org. Chem.* **2004**, *1*, 403−415.
(6) Wang, P.; Song, Y.; Zhang, L.; He, H.; Zhou, X. *Curr. Med. Chem.* **2005**, *12*, 2893−2913.
(7) Wang, H. *Curr. Org. Chem.* **2014**, *18*, 44−60.
(8) Rokita, S. E.; Yang, J.; Pande, P.; Greenberg, W. A. *J. Org. Chem.* **1997**, *62*, 3010−3012.
(9) Veldhuyzen, W. F.; Shallop, A. J.; Jones, R. A.; Rokita, S. E. *J. Am. Chem. Soc.* **2001**, *123*, 11126−11132.
(10) Weinert, E. E.; Frankenfield, K. N.; Rokita, S. E. *Chem. Res. Toxicol.* **2005**, *18*, 1364−1370.
(11) Chatterjee, M.; Rokita, S. E. *J. Am. Chem. Soc.* **1994**, *116*, 1690−1697.
(12) Zeng, Q.; Rokita, S. E. *J. Org. Chem.* **1996**, *61*, 9080−9081.
(13) Pande, P.; Shearer, J.; Yang, J.; Greenberg, W. A.; Rokita, S. E. *J. Am. Chem. Soc.* **1999**, *121*, 6773−6779.
(14) Veldhuyzen, W. F.; Pande, P.; Rokita, S. E. *J. Am. Chem. Soc.* **2003**, *125*, 14005−14013.
(15) McCracken, P. G.; Bolton, J. L.; Thatcher, G. R. J. *J. Org. Chem.* **1997**, *62*, 1820−1825.
(16) Modica, E.; Zanaletti, R.; Freccero, M.; Mella, M. *J. Org. Chem.* **2001**, *66*, 41−52.
(17) Arumugam, S.; Guo, J.; Mbua, N. E.; Friscourt, F.; Lin, N.; Nekongo, E.; Boons, G.-J.; Popik, V. V. *Chem. Sci.* **2014**, *5*, 1591−1598.
(18) Kralj, M.; Uzelac, L.; Wang, Y.-H.; Wan, P.; Tireli, M.; Mlinarić-Majerski, K.; Piantanida, I.; Basarić, N. *Photochem. Photobiol. Sci.* **2015**, *14*, 1082−1092.
(19) Basarić, N.; Mlinarić-Majerski, K.; Kralj, M. *Curr. Org. Chem.* **2014**, *18*, 3−18.
(20) Percivalle, C.; Doria, F.; Freccero, M. *Curr. Org. Chem.* **2014**, *18*, 19−43.
(21) Colloredo-Mels, S.; Doria, F.; Verga, D.; Freccero, M. *J. Org. Chem.* **2006**, *71*, 3889−3895.
(22) Škalamera, Đ.; Bohne, C.; Landgraf, S.; Basarić, N. *J. Org. Chem.* **2015**, *80*, 10817−10828.
(23) Doria, F.; Lena, A.; Bargiggia, R.; Freccero, M. *J. Org. Chem.* **2016**, *81*, 3665−3673.
(24) Diao, L.; Yang, C.; Wan, P. *J. Am. Chem. Soc.* **1995**, *117*, 5369−5370.
(25) Arumugam, S.; Popik, V. V. *J. Am. Chem. Soc.* **2009**, *131*, 11892−11899.
(26) Verga, D.; Nadai, M.; Doria, F.; Percivalle, C.; Di Antonio, M.; Palumbo, M.; Richter, S. N.; Freccero, M. *J. Am. Chem. Soc.* **2010**, *132*, 14625−14637.
(27) Doria, F.; Richter, S. N.; Nadai, M.; Colloredo-Mels, S.; Mella, M.; Palumbo, M.; Freccero, M. *J. Med. Chem.* **2007**, *50*, 6570−6579.
(28) Nadai, M.; Doria, F.; Di Antonio, M.; Sattin, G.; Germani, L.; Percivalle, C.; Palumbo, M.; Richter, S. N.; Freccero, M. *Biochimie* **2011**, *93*, 1328−1340.
(29) Doria, F.; Nadai, M.; Folini, M.; Di Antonio, M.; Germani, L.; Percivalle, C.; Sissi, C.; Zaffaroni, N.; Alcaro, S.; Artese, A.; Richter, S. N.; Freccero, M. *Org. Biomol. Chem.* **2012**, *10*, 2798−2806.
(30) Doria, F.; Nadai, M.; Folini, M.; Scalabrin, M.; Germani, L.; Sattin, G.; Mella, M.; Palumbo, M.; Zaffaroni, N.; Fabris, D.; Freccero, M.; Richter, S. N. *Chem. - Eur. J.* **2013**, *19*, 78−81.
(31) Di Antonio, M.; Doria, F.; Mella, M.; Merli, D.; Profumo, A.; Freccero, M. *J. Org. Chem.* **2007**, *72*, 8354−8360.
(32) Percivalle, C.; La Rosa, A.; Verga, D.; Doria, F.; Mella, M.; Palumbo, M.; Di Antonio, M.; Freccero, M. *J. Org. Chem.* **2011**, *76*, 3096−3106.
(33) Škalamera, Đ.; Mlinarić-Majerski, K.; Martin-Kleiner, I.; Kralj, M.; Wan, P.; Basarić, N. *J. Org. Chem.* **2014**, *79*, 4390−4397.
(34) Basarić, N.; Žabčić, I.; Mlinarić-Majerski, K.; Wan, P. *J. Org. Chem.* **2010**, *75*, 102−116.
(35) Basarić, N.; Cindro, N.; Bobinac, D.; Mlinarić-Majerski, K.; Uzelac, L.; Kralj, M.; Wan, P. *Photochem. Photobiol. Sci.* **2011**, *10*, 1910−1925.
(36) Basarić, N.; Cindro, N.; Bobinac, D.; Uzelac, L.; Mlinarić-Majerski, K.; Kralj, M.; Wan, P. *Photochem. Photobiol. Sci.* **2012**, *11*, 381−396.
(37) Veljković, J.; Uzelac, L.; Molčanov, K.; Mlinarić-Majerski, K.; Wan, P.; Basarić, N. *J. Org. Chem.* **2012**, *77*, 4596−4610.
(38) Rochlin, E.; Rappoport, Z. *J. Org. Chem.* **2003**, *68*, 216−226.
(39) Lee, J.; Robinson, G. W.; Webb, S. P.; Philips, L. A.; Clark, J. H. *J. Am. Chem. Soc.* **1986**, *108*, 6538−6542.
(40) Robinson, G. W. *J. Phys. Chem.* **1991**, *95*, 10386−10391.
(41) Tolbert, L. M.; Haubrich, J. E. *J. Am. Chem. Soc.* **1994**, *116*, 10593−10600.
(42) Solntsev, K. M.; Huppert, D.; Agmon, N.; Tolbert, L. M. *J. Phys. Chem. A* **2000**, *104*, 4658−4669.
(43) Montalti, M.; Credi, A.; Prodi, L.; Gandolfi, M. T. In *Handbook of Photochemistry*; CRC Taylor and Francis: Boca Raton, 2006.
(44) Krohn, K.; Rieger, H.; Khanbabaee, K. *Chem. Ber.* **1989**, *122*, 2323−2330.
(45) Goldstein, S.; Rabani, J. *J. Photochem. Photobiol., A* **2008**, *193*, 50−55.
(46) Kuhn, H. J.; Braslavsky, S. E.; Schmidt, R. *Pure Appl. Chem.* **2004**, *76*, 2105−2146.
(47) Kulikov, A.; Arumugam, S.; Popik, V. V. *J. Org. Chem.* **2008**, *73*, 7611−7615.
(48) Arumugam, S.; Popik, V. V. *J. Am. Chem. Soc.* **2011**, *133*, 5573−5579.
(49) Van De Water, R.; Pettus, T. R. R. *Tetrahedron* **2002**, *58*, 5367−5405.
(50) Arumugam, S.; Popik, V. V. *J. Am. Chem. Soc.* **2012**, *134*, 8408−8411.
(51) Albrecht, M.; Bohne, C.; Granzhan, A.; Ihmels, H.; Pace, T. C. S.; Schnurpfeil, A.; Waidelich, M.; Yihwa, C. *J. Phys. Chem. A* **2007**, *111*, 1036−1044.
(52) Olmsted, J., III *J. Phys. Chem.* **1979**, *83*, 2581−2584.
(53) Boens, N.; Basarić, N.; Novikov, E.; Crovetto, L.; Orte, A.; Talavera, E. M.; Alvarez-Pez, J. M. *J. Phys. Chem. A* **2004**, *108*, 8180−8189.
(54) Qin, W.; Basarić, N.; Boens, N. *J. Phys. Chem. A* **2005**, *109*, 4221−4230.
(55) Fischer, M.; Wan, P. *J. Am. Chem. Soc.* **1999**, *121*, 4555−4562.
(56) Chiang, Y.; Kresge, A. J.; Zhu, Y. *J. Am. Chem. Soc.* **2000**, *122*, 9854−9855.
(57) Chiang, Y.; Kresge, A. J.; Zhu, Y. *J. Am. Chem. Soc.* **2001**, *123*, 8089−8094.
(58) Dixon, W. T.; Murphy, D. *J. Chem. Soc., Faraday Trans. 2* **1976**, *72*, 1221−1230.
(59) Bordwell, F. G.; Cheng, J.-P. *J. Am. Chem. Soc.* **1991**, *113*, 1736−1743.
(60) Kleinman, M. H.; Flory, J. H.; Tomalia, D. A.; Turro, N. J. *J. Phys. Chem. B* **2000**, *104*, 11472−11479.
(61) Pretali, L.; Doria, F.; Verga, D.; Profumo, A.; Freccero, M. *J. Org. Chem.* **2009**, *74*, 1034−1041.
(62) Gadosy, T. A.; Shukla, D.; Johnston, L. J. *J. Phys. Chem. A* **1999**, *103*, 8834−8839.
(63) Agmon, N. *J. Phys. Chem. A* **2005**, *109*, 13−35.
(64) Brousmiche, D.; Xu, M.; Lukeman, M.; Wan, P. *J. Am. Chem. Soc.* **2003**, *125*, 12961−12970.
(65) McClelland, R. A.; Chan, C.; Cozens, F. L.; Modro, A.; Steenken, S. *Angew. Chem., Int. Ed. Engl.* **1991**, *30*, 1337−1339.
(66) Cozens, F. L.; Kanagasabapathy, V. M.; McClelland, R. A.; Steenken, S. *Can. J. Chem.* **1999**, *77*, 2069−2082.
(67) Sargent, F. P.; Gardy, E. M. *Chem. Phys. Lett.* **1976**, *39*, 188−190.
(68) Boyle, J. V.; Ghormley, J. A.; Hochanadel, C. H.; Riley, J. F. *J. Phys. Chem.* **1969**, *73*, 2886−2890.
(69) Buxton, G. V.; Greenstock, C. L.; Helman, W. P.; Ross, A. B. *J. Phys. Chem. Ref. Data* **1988**, *17*, 513−886.

DOI: 10.1021/acs.joc.6b02735
J. Org. Chem. 2017, 82, 6006−6021

(70) Vauthey, E.; Haselbach, E.; Suppan, P. *Helv. Chim. Acta* **1987**, *70*, 347−353.
(71) Yang, N. C.; Libman, J. *J. Am. Chem. Soc.* **1973**, *95*, 5783−5784.
(72) Bohne, C.; Kennedy, S. R.; Boch, R.; Negri, F.; Orlandi, G.; Siebrand, W.; Scaiano, J. C. *J. Phys. Chem.* **1991**, *95*, 10300−10306.
(73) Neta, P.; Grodkowski, J. *J. Phys. Chem. Ref. Data* **2005**, *34*, 109−199.
(74) Schuler, R. H. *Radiat. Res.* **1977**, *69*, 417−433.
(75) Hunter, E. P. L.; Desrosiers, M. F.; Simic, M. G. *Free Radical Biol. Med.* **1989**, *6*, 581−585.
(76) Ferrari, J. L.; Hunsberger, I. M.; Gutowsky, H. S. *J. Org. Chem.* **1960**, *25*, 485−486.
(77) Ferrari, J. L.; Hunsberger, I. M.; Gutowsky, H. S. *J. Am. Chem. Soc.* **1965**, *87*, 1247−1255.
(78) Liao, Y.; Bohne, C. *J. Phys. Chem.* **1996**, *100*, 734−743.
(79) Mitchell, R. H.; Bohne, C.; Wang, Y.; Bandyopadhyay, S.; Wozniak, C. B. *J. Org. Chem.* **2006**, *71*, 327−336.

DOI: 10.1021/acs.joc.6b02735
J. Org. Chem. 2017, 82, 6006−6021